Two-dimensional electron density of states in a transverse magnetic field

I. V. Kukushkin, S. V. Meshkov, and V. B. Timofeev

Solid State Physics Institute, Academy of Sciences of the USSR, Chernogolovka (Moscow region)

Usp. Fiz. Nauk **155**, 219–264 (June 1988)

This review covers the current theoretical concepts and experimental methods employed in studying the two-dimensional electron density of states in a magnetic field. The authors discuss the different factors that determine the energy distribution of the density of states in real systems. They demonstrate the importance of the screening of random external potential fluctuations by two-dimensional electrons and particularly the oscillatory dependence of screening on electron concentration. When considering the various theoretical approaches and experimental methods, the authors analyze their conditions of applicability and the self-consistency of obtained results. They demonstrate that it is possible to evaluate experimentally the random potential amplitude and range from the oscillations in Landau level broadening.

TABLE OF CONTENTS

1. INTRODUCTION

In semiconductors quasi-two-dimensional electron or hole space-charge layers appear in channels located at the interfaces in heterojunctions and metal-insulator-semiconductor (MIS) structures.[1] In these channels electron motion normal to the interface (along the z-axis) is constrained by a narrow potential well, leading to a discrete electron spectrum in this direction. The electron gas can be considered two-dimensional (2D-) if the energy scale associated with the transverse quantization in the channel exceeds all other characteristic energies of the electronic system (the Fermi energy E_F, temperature T, cyclotron energy $\hbar\omega_c$, etc.).

Two-dimensional electronic structures have attracted great attention in recent years not only because of their varied and important applications in microelectronics, but also because of the discovery of a fundamentally new phenomenon—the quantum Hall effect (QHE), both integral[2] and fractional.[3] For this discovery Klaus von Klitzing was awarded the 1988 Nobel Prize in physics. The quantum Hall effect (see review article [4]) occurs only in two-dimensional systems. In order to understand it on a microscopic level it is essential to know the energy spectrum of 2D-electrons $D(E)$ in a transverse magnetic field, taking into account the random defect potential present in real structures and the screening of this potential by 2D-electrons.

When a transverse magnetic field H is applied to an ideal 2D-electron gas the energy spectrum becomes fully discrete because orbital motion in the plane of the layer (x,y) is quantized-by the field:

$$E_N = \hbar\omega_c\left(N+\frac{1}{2}\right);$$

where $\omega_c = eH/m_c$ is the cyclotron frequency, m_c is the effective mass, N is a quantum number. The density of states (DS) in such a system consists of a series of equally spaced δ-functions separated by $\hbar\omega_c$. The electrons present in the system fill these Landau levels from the lowest level up. The number of electron-containing levels is denoted by the filling factor ν, which is determined by the ratio of the electron concentration n_S to the Landau level degeneracy per unit area $(2\pi l_H^2)^{-1}$ ($l_H = (\hbar/eH)^{1/2}$ is the magnetic length):

$$\nu = 2\pi l_H^2 n_S = \frac{n_S h}{eH}.$$

In real 2D-systems electrons are influenced by a random potential produced by various defects (interface roughness, charged impurity centers near the inversion layer, etc.). Interaction with this random potential lifts the degeneracy and the Landau levels acquire a finite width. The distribution of a single-particle density of states is determined by the types of inhomogeneities present, as well as the screening of their random potential. The screening, in turn, depends on the filling factor ν. Studies of the DS as a func-

 0038-5670/88/060511-24$01.80

tion of magnetic field and filling factor yield valuable information on the range and amplitude of inhomogeneities in real 2D-systems. In particular, this information is essential for the understanding of magnetotransport in two-dimenstional space-charge layers in a wide range of level filling by charge carriers.

To date, various experimental methods have been tried for measuring the density of states of 2D-systems in a transverse magnetic field. Most of these methods measured the so-called thermodynamic density of states $D_T(E_F) = dns/dE_F$, which characterizes the integrated energy spectrum. This quantity was deduced from the oscillatory behavior of such thermodynamic quantities as magnetization,[8] electronic heat capacity,[6] and also using thermally activated transport.[7] It turned out that $D_T(E_F)$ exhibits a fairly sharp peak near half-integral filling factors whose width is in good agreement with estimated carrier mobilities (see Ref. 1), but the DS does not become exponentially small between Landau levels. This phenomenon was treated as a "plateau" that formed a background to the Gaussian-shaped DS peaks and various theories explaining the formation of this plateau were proposed. Still, the observed DS behavior could only be interpreted by invoking random potential screening that oscillates with the filling factor ν.

The single-particle density of states $D(E)$ can also be studied by the spectroscopic method[8] based on spectral luminescence measurements of 2D-electrons. The spectroscopic method makes it possible to determine how the energy spectrum is affected by the screening of random potential fluctuations and to gather information on the amplitude and range of the random potential itself.

In this review we consider all the above topics. We analyze both the theoretical aspects of random potential properties that affect the densities of states of 2D-systems and the experimental results of DS measurements in a transverse magnetic field obtained by various means.

2. THEORETICAL CONCEPTS

First let us consider a number of questions related to the very idea of the density of states. In the simplest case of an ideal Fermi gas the problem reduces to finding the energy spectrum (i.e. solving the Schrödinger equation) of a single particle in a random potential. By definition, given a system that occupies a sufficiently large area the number of states per unit energy interval and unit area averages out to the density of states $D(E)$. This quantity does not depend on temperature or the position of the Fermi level E_F; it is related to the carrier concentration n_S in a 2D-system by the integral

$$n_S(E_F) = \int_0^\infty D(E) \left(\exp\frac{E-E_F}{kT} + 1\right)^{-1} dE. \qquad (2.1)$$

The thermodynamic density of states $D_T(E_F) = dn_S/dE_F$ equals the value of $D(E)$ at the Fermi level at $T = 0$.

When electron-electron interaction is taken into account the energy spectrum of a many-particle system becomes exceedingly complex and, strictly speaking, unrelated to the spectrum of a single particle. In this case, the single-particle density of states at any temperature is determined by the imaginary part of a retarded Green's function collapsed over the coordinates and averaged over the random potential realizations

$$D(E) = S^{-1} \operatorname{Sp} \operatorname{Im} \hat{G}(E).$$

For an ideal gas this quantity concides with definition (2.1). When particle-particle interactions are taken into account, however, $D(E)$ becomes parametrically dependent on E_F and T. This is the fundamental characteristic of the energy spectrum of many-particle systems. A powerful method using Green's functions with diagram techniques exists for computing $D(E)$.[9] In particular, this method has been adapted for magnetic field calculations.[10] In certain conditions it accommodates direct experimental optical measurements (applications to 2D-systems are discussed in Sec. 4 of this review).

The relation (2.1) between $D(E)$ and concentration n_S holds for all values of T and E_F even when particle interactions are taken into account, but since $D(E)$ now depends on the position of the Fermi level $D_T(E_F)$ no longer coincides with $D(E_F)$ at zero temperature.

A consistent calculation of electron-electron interactions by perturbation theory methods generally assumes that the Coulomb energy at the characteristic distance between electrons is small compared to the broadening of their energy distribution. In a magnetic field a measure of the interaction's weakness is usually taken as the ratio of the magnetic length to the Bohr radius $a^* = \varkappa\hbar^2/me^2$ ($\varkappa$ is the permittivity of the medium). In reality the ration l_H/a^* is not small ($\geqslant 1$ for heterostructures and $\geqslant 3$ for MIS-structures) and electron-electron interaction effects can be significant. In particular, electron-electron interaction should broaden the Landau levels because of quasiparticle decay, just as in an ordinary Fermi liquid[9] (this decay is forbidden in the highest occupied Landau level because of energy constraints, but in the lower-lying levels it is small only according to the parameter l_H/a^*).

A rigorous analysis of the electron-electron interaction is crucial in treating the ground state of a two-dimensional electron system at fractional filling factors. Many such calculations, which we shall not discuss, have been performed in the course of studying the fractional QHE.[4]

Currently the only practical approach for quantitatively studying the two-dimensional Landau levels in a random potential involves the self-consistent field approximation. The self-consistent potential is made up of the original random potential and the electrostatic potential arising from the spatial redistribution of electrons; when calculating the level broadening and charge density in this potential the electrons are treated as noninteracting. The errors arising in the self-consistent field method from neglecting correlation and Fermi liquid effects are probably insignificant compared to the additional approximations that are usually employed. There are no experimental indications of any significant renormalizations of measured physical properties, and this also gives grounds for optimism.

Below we shall list the currently available theoretical results pertaining to the single-particle density of states. First, we consider several practically important random potential models. Second, in order of ascending difficulty, we consider level broadening in the absence of electron-electron interaction, linear screening of a weak random potential,

and, finally, the nonlinear effects that occur when level broadening becomes comparable to inter-level spacing. Most of the cited theoretical studies analyze the questions pertaining to the single-particle density of states $D(E)$, i.e. to the width and shape of the Landau levels at a fixed filling factor ν. The thermodynamic density of states is usually estimated from the semiqualitative considerations set out in Sec. 2.4.

When discussing the literature we shall give preference to analytical results and qualitative ideas that shed light on the physical picture. Studies devoted to numerical realization of complicated self-consistent calculations shall get brief mention only.

2.1. Random potentials

Spatial inhomogeneities present in real 2D-channels differ both in their physical origin and in their contribution to the effective random potential. Crystal structure imperfections and, probably, surface roughness create a relatively short-range potential whose quantitative properties are largely unknown. One of the more experimentally important sources of the random potential is the charged impurity center distribution in the vicinity of the channel. The long-range Coulomb potentials of charged centers overlap and add up to a smooth random potential with a long characteristic length.

We shall restrict our attention to Gaussian-type random potentials discussed in most theoretical studies. In addition to their simple correlation properties that make for easier calculations such potentials are important for purely physical reasons: they result from the overlapping potentials of a large number of weak, randomly distributed scattering sources. For example, the potential created in the plane of the channel by Coulomb centers is Gaussian to good accuracy on the scale of the order of or greater than their separation.

A general property of random Gaussian potentials is their symmetry: that is, they are equally likely to go above or below the mean value. Potentials created by strong, short-range scatterers, nonsymmetric, but this appears to be principally important only in studies of two-dimensional channel mobility, cyclotron resonance, and the like. For Landau level broadening calculations these factors can be modelled by short-range Gaussian potentials with sufficient accuracy. The symmetry of Gaussian potentials poses no problem in this case because so far very few experiments[12] have indicated an asymmetric density of states about the mean positions of the Landau levels.

The random Gaussian potential in the plane of the channel $U(\mathbf{r})$ with a mean value of zero is completely described by the pair correlator

$$Q(\mathbf{r}-\mathbf{r}') \equiv \langle U(\mathbf{r})\, U(\mathbf{r}')\rangle$$

($\mathbf{r}$ is the two-dimensional radius vector). The Fourier transform of this correlator

$$Q_{\mathbf{k}} \equiv \int Q(\mathbf{r}) \exp(-i\mathbf{kr})\, \mathrm{d}^2 r$$

determines the Fourier component distribution of the potential:

$$\langle U_{\mathbf{k}} U_{\mathbf{k}'}\rangle = (2\pi)^2 \delta(\mathbf{k}+\mathbf{k}')\, Q_{\mathbf{k}},$$
$$U_{\mathbf{k}} \equiv \int U(\mathbf{r}) \exp(-i\mathbf{kr})\, \mathrm{d}^2 r.$$

An important characteristic of the random potential is its dispersion, i.e., the mean-square value Γ:

$$\Gamma^2 = \langle U(\mathbf{r})\, U(\mathbf{r})\rangle = \int Q_{\mathbf{k}} \frac{\mathrm{d}^2 k}{(2\pi)^2}. \tag{2.2}$$

A mathematically Gaussian random potential is defined as a potential in which the probability of a random fluctuation $u(r)$ is proportional to

$$\exp\left(-\int U(\mathbf{r})\, Q^{-1}(\mathbf{r}-\mathbf{r}')\, U(\mathbf{r}')\, \mathrm{d}^2 r\, \mathrm{d}^2 r'\right),$$

where $Q^{-1}(\mathbf{r}-\mathbf{r}')$ operator is the inverse of $Q(\mathbf{r}-\mathbf{r}')$, and hence has Fourier components $Q_{\mathbf{k}}^{-1}$.

A concentration $n(\mathbf{R})$ of scatterers randomly distributed in space ($\mathbf{R} \equiv \{\mathbf{r}, z\}$ is the three-dimensional radius vector) creates a random potential with the correlator

$$\langle U(\mathbf{R})\, U(\mathbf{R}')\rangle = \int V(\mathbf{R}, \mathbf{R}_0)\, V(\mathbf{R}', \mathbf{R}_0)\, n(\mathbf{R}_0)\, \mathrm{d}^3 R_0$$
$$-\left(\int V(\mathbf{R}, \mathbf{R}_0)\, n(\mathbf{R}_0)\, \mathrm{d}^3 R_0\right)\left(\int V(\mathbf{R}', \mathbf{R}_0)\, n(\mathbf{R}_0)\, \mathrm{d}^3 R_0\right), \tag{2.3}$$

where $V(\mathbf{R}, \mathbf{R}_0)$ is the potential at point $\mathbf{R}$ due to a scatterer located at $\mathbf{R}_0$. If the distribution of scatterers $n(z)$ is homogenous in the plane

$$Q_{\mathbf{k}} = \int \left| \int V(\mathbf{R}, \mathbf{R}_0) \exp(-i\mathbf{kr})\, \mathrm{d}^2 r \right|^2 n(z_0)\, \mathrm{d}z_0.$$

We emphasize that the characteristic length scale of the potential correlations is determined solely by the properties of the scatterers and does not depend on their concentration. The extent to which the resulting potential is indeed Gaussian does depend on the scatterer concentration, however.

Now let us describe several practical random two-dimensional potentials. The simplest and most conventient potential (because it does not diverge in the long wavelength limit and falls off quickly at short wavelengths) has a Gaussian correlator:

$$Q(\mathbf{r}) = \Gamma^2 \exp\left(-\frac{r^2}{2d^2}\right), \quad Q_{\mathbf{k}} = 2\pi d^2 \Gamma^2 \exp\left(-\frac{k^2 d^2}{2}\right). \tag{2.4}$$

According to (2.3) this purely theoretical potential can arise from a randomly distributed collection of scatterers with individual potentials $V(\mathbf{R},\mathbf{R}_0) \sim \exp[-(\mathbf{R}-\mathbf{R}_0)^2/d^2]$. Hopefully, given the appropriate choice of parameters, the correlator (2.4) can adequatly describe the effective potential created by surface roughness. Another frequently used "white-noise" potential consists of a Gaussian potential with the correlator

$$Q(\mathbf{r}) = w\delta(\mathbf{r}), \quad Q_{\mathbf{k}} = w = \mathrm{const}$$

which can be treated as the limiting form of potential (2.3) with a small correlation length but high dispersion:

$$d \to 0, \quad (2\pi)^{1/2} \Gamma d \to w.$$

Potentials created by randomly distributed charged centers usually exhibit a power-law dependence of the correlator Q_k in a wide range of wavelengths. The details of this dependence are determined by the distribution of impurities in the perpendicular direction to the channel $n(z)$, by the inhomogeneity of the permittivity in this same direction

$\varkappa(z)$, by the presence of a metallic electrode (gate), and so forth (everything is taken to be homogenous in the channel plane). When all these factors are taken into account, the general form of the random potential correlator in the $z = 0$ channel plane

$$Q_{\mathbf{k}} = \int G_{\mathbf{k}}^2(0, z_0)\, n(z_0)\, dz_0,$$

is expressed via the Green's function $G_{\mathbf{k}}(z,z_0)$ of the Poisson equation, i.e., the solution of

$$\varkappa(z)\left(\frac{d^2G}{dz^2} - k^2G\right) + \frac{dG}{dz}\frac{d\varkappa(z)}{dz} = -4\pi\delta(z - z_0),$$

that decreases as $z \to \pm\infty$. The presence of a conducting electrode is formally equivalent to setting $\varkappa(z)$ to infinity at the appropriate value of z.

We now list the simplest and most common cases drawn from the various semiconductor systems in which two-dimensional channels have been realized. Singly charged centers uniformly distributed in the homogenous medium with concentration n_3 create a random potential in the $z = 0$ plane that has the correlator

$$Q_{\mathbf{k}} = \frac{4\pi^2e^4n_3}{\varkappa^2k^3}. \tag{2.5}$$

These same centers, distributed in the plane of the channel with a two-dimensional concentration n_2, yield a correlator

$$Q_{\mathbf{k}} = \frac{4\pi^2e^4n_2}{\varkappa^2k^2} \tag{2.6}$$

which contains fewer long wavelength harmonics and more short wavelength ones. In both cases the dispersion (2.2) of the potential is infinits, but for correlator (2.5) integral (2.2) diverges at the lower limit by a power law, whereas for correlator (2.6) the divergence of (2.2) is logarithmic at both limits.

Typically, in heterostructures there exists a charge-free (spacer) layer of thickness h near the channel, which leads to an exponentially decreasing correlator in the short wavelength region:

$$Q_{\mathbf{k}} = \frac{4\pi^2e^4n_3}{\varkappa^2k^3}\exp(-2kh), \quad Q_{\mathbf{k}} = \frac{4\pi^2e^4n_2}{\varkappa^2k^2}\exp(-2kh).$$

Taking the finite width of the channel into account should have approximately the same effect.

In MIS-systems the permittivities of the semiconductor $\varkappa_s$ and the insulator $\mathbf{k}_d$ (where most of the charges are located) are typically different. A screening metallic electrode is usually present as well. Then, correlators (2.5) and (2.6) take the form

$$Q_{\mathbf{k}} = \frac{2\pi^2e^4n_3}{\bar{\varkappa}^2k^3}\,\frac{1 - 4kh\exp(-2kh) - \exp(-4kh)}{[1 - (\varkappa_s - \varkappa_d)(\varkappa_s + \varkappa_d)^{-1}\exp(-2kh)]^2}, \tag{2.7a}$$

$$Q_{\mathbf{k}} = \frac{4\pi^2e^4n_2}{\bar{\varkappa}^2k^2}\left[\frac{1 - \exp(-2kh)}{1 - (\varkappa_s - \varkappa_d)(\varkappa_s + \varkappa_d)^{-1}\exp(-2kh)}\right]^2, \tag{2.7b}$$

where $\bar{\varkappa} = (\varkappa_s + \varkappa_d)/2$, h is the insulator thickness, n_3 is the charge concentration in the insulator. The short wavelength divergence disappears and the dispersion (2.2) of the potential created by spatially distributed charges (2.7a) becomes finite (using silicon paramters: $\varkappa_s = 11.5$, $\varkappa_d = 3.9$, $\Gamma \approx 4.1(10^{-10}\ \mathrm{cm}^2 n_3 h)^{1/2}$ MeV). A correlation in the spatial impurity distribution has a similar effect.

2.2. Noninteracting electrons

The single-particle solution of the Landau level broadening problem is probably the simplest possible and is currently well known. However, the conditions a real system must satisfy in order for this solution to hold are quite stringent. In order to neglect electron-electron interaction not only must the parameter satisfy $l_H/a^* \ll 1$, but the screening of the random potential must be weak, which happens only at integral filling factors ν (see Sec. 2.3). Moreover, the level broadening must be small compared to inter-level spacing, for otherwise potential screening becomes significant even at integral ν (see Sec. 2.4). Even though the above conditions usually cannot be satisfied, the single-particle approximation results for the shape and broadening of the Landau levels and their dependence on the nature of the random potential are still of certain interest.

In the absence of electron-electron interaction, the perturbation picture of the electron Green's function consists of a sequence of unifilar, i.e., loop-less, diagrams containing different impurity lines. If the level broadening is small zero-order approximation Green's functions can be taken to belong to the same level. The phase multipliers that appear at intersections of impurity lines make the summing of diagrams difficult in the general case, and all computations employ additional approximations of one sort or another.

The first step in this direction were studies by Ando,[13] which simply omitted inconvenient diagrams with intersecting impurity lines without any practical justification. The resulting so-called self-consistent Born approximation yields DS peaks of a semielliptical shape. For the Nth level the density of states

$$2\pi l_H^2 D(E) = (2\pi\Gamma_N)^{-1}\left[1 - \left(\frac{E}{2\Gamma_N}\right)^2\right]^{1/2}, \quad |E| < 2\Gamma_N, \tag{2.8}$$

is finite in a finite energy interval and turns to zero elsewhere. The width Γ_N is expressed via the random potential correlator:

$$\Gamma_N^2 = \int Q_{\mathbf{k}}\exp\left(-\frac{k^2l_H^2}{2}\right)\left[L_N\left(\frac{k^2l_H^2}{2}\right)\right]^2\frac{d^2k}{(2\pi)^2}$$

$$= \int Q(\mathbf{r})\exp\left(-\frac{r^2}{2l_H^2}\right)\left[L_N\left(\frac{r^2}{2l_H^2}\right)\right]^2\frac{d^2r}{2\pi l_H^2}, \tag{2.9}$$

where L_N is a Laguerre polynomial. Energy is reckoned from the positions of the unbroadened Nth Landau level.

The physically unrealistic sharp edges in the density of states (2.8) emphasize the crudeness of the self-consistent Born approximation. The actual shape of a Landau level depends on the ratio of the random potential range d (for correlators similar to (2.4)) to the magnetic length l_H, as well as on the level number N. We now describe the results pertaining to various limiting cases.

1) In the smooth potential limit $d \gg l_H$ the integrals in the diagrams occur in the low momentum region and phase multipliers can be neglected. In this case diagrams can be trivially summed and the levels are Gaussian:

$$2\pi l_H^2 D(E) = \frac{\Gamma_N^{-1}}{(2\pi)^{1/2}}\exp\left(-\frac{E^2}{2\Gamma_N^2}\right).$$

This result was obtained by Gerhardts[14] by the method of cumulant expansion. Hikami and Brezin[15] went further and obtained the first few terms of $D(E)$ expanded in powers of

the inverse correlation length. Their results, however, lie outside the bounds of applicability of the noninteracting electron approximation (see Sec. 2.3).

2) In the opposite limit $d \ll l_H$ that applies to higher Landau levels $N \gg 1$ another simplification occurs:[16] the phase multipliers begin to oscillate rapidly and diagrams that contain these multipliers can be neglected. In this limit, therefore, the self-consistent Born approximation becomes entirely valid and leads to the result (2.8) with level width

$$\Gamma_N^2 = \int Q(r)\,(2\pi l_H^2)^{-1}\,\mathrm{d}^2 r = \frac{w}{2\pi l_H^2}, \qquad (2.10)$$

which is the same for all levels and proportional to the white noise intensity w. Given a short-range random potential, the shape of a level tends towards the semielliptic form as the level number increases, as was demonstrated numerically by Ando.[17]

3) In the white noise limit $d \gg l_H$, Wegner[18] and then Brezin and co-workers[19] obtained an exact analytic solution for the ground level $N = 0$:

$$2\pi l_H^2 D(E) = 2\,(\pi^{3/2}\gamma)^{-1} \exp\left(\frac{E}{\gamma}\right)^2 \times\left[1+\left(2\pi^{-1/2}\int_0^{E/\gamma}\exp x^2\,\mathrm{d}x\right)^2\right]^{-1}, \qquad (2.11)$$

$$\gamma^2 = \frac{w}{2\pi l_H^2},$$

γ coincides with the level width (2.10).

4) Exponential (Lifshits) tails of the density of states $D(E)$ in the $\hbar\omega_c \gg |E| \gg \Gamma_N$ region have been studied in the white noise limit only.[20-22] They are of paramount importance in the $d \ll l_H$, $N \gg 1$ case, when the "core" of the level exhibits square-root edges in the density of states at $|E| = 2\Gamma_N$. The optimal fluctuation method yields

$$2\pi l_H^2 D(E) = C_N E^2 \gamma_N^{-3} \exp\left(-\frac{E^2}{\gamma_N^2}\right),$$

$$\gamma_N^2 = \frac{w}{2\pi l_H^2}\,\frac{(2N-1)!!}{(2N)!!}.$$

The numerical coefficient C_N in the preexponential factor has been obtained for the ground state as $C_0 = \pi\sqrt{2}$,[21] which agrees with the exact solution (2.11) (the value cited in Ref. 20 is smaller by a factor of two). Asymptotic values of C_N for high level numbers $N \gg 1$ have also been calculated.[21]

Summarizing the above results, we note that expression (2.9) yields the correct value for the mean-square width of the Landau level both in the $d \gg l_H$ limit and in the opposite limit (the shape of the density of states peak strongly depends on the relation between d and l_H). Therefore, expression (2.9) can at the very least serve as a good interpolation formula for an arbitrary Gaussian potential.

An interesting property of this expression is that the width of all Landau levels becomes the same both in the smooth potential limit and in the opposite, white noise limit because of the $L_N(0) = 1$ equality. This can be emphasized by considering the analytic expression for Γ_N given a Gaussian correlator (2.4):

$$\Gamma_N^2 = \frac{\Gamma^2 d^2}{d^2 + l_H^2}\left(\frac{d^2 - l_H^2}{d^2 + l_H^2}\right)^N P_N\left(\frac{d^4 - l_H^4}{d^4 + l_H^4}\right),$$

where P_N is the Legendre polynomial. In the case of a smooth potential $d \gg l_H$ the equal width of the levels is a natural consequence of independent local energy shifts of large regions in the system. The width of the levels Γ_N then matches the dispersion of the random potential, $\Gamma = (\langle U^2(\mathbf{r})\rangle)^{1/2}$. In the white noise limit $d \ll l_H$ the equal broadening of different levels is nontrivial and no simple physical interpretation has been offered to date.

In the $d \ll l_H$ limit (see, for example, Ref. 23) the level broadening (2.9) is simply related to the $H = 0$ electron mobility μ calculated for the same channel in the Born approximation:

$$\Gamma_N = \hbar\omega_c\left(\frac{\pi\mu H}{2}\right)^{-1/2},$$

but this relation is probably due to the formally analogous integrals that enter in the expressions for Γ and μ.

2.3. Linear screening

In the linear response approximation the screening properties of 2D-electron gas are described by its permittivity $\tilde{\varkappa}(\mathbf{k})$. This function describes, as is usual, the factor by which the polarization of the 2D-system reduces the different (two-dimensional) harmonics of the external potential. Linear screening does not affect the Gaussian nature of the random potential: the correlator $\tilde{Q}_k$ of the self-consistent potential is obtained when the correlator $\tilde{Q}_k$ of the external potential is divided by the square of the permittivity $\tilde{Q}_k = Q_k/\tilde{\varkappa}^2(\mathbf{k})$.

In the absence of a magnetic field the dependence $\tilde{\varkappa}(\mathbf{k})$ is well known (see, for example, Ref. 4). When the temperature is small compared to E_F,

$$\tilde{\varkappa}(\mathbf{k}) = 1 + \frac{2g_v}{ka^*}, \quad k \leqslant 2k_F,$$

$$= 1 + \frac{2g_v}{ka^*}\left\{1 - \left[1 - \left(1 - \frac{2k_F}{k}\right)^2\right]^{1/2}\right\}, \quad k > 2k_F, \qquad (2.12)$$

where $2g_v$ is the full multiplicity of the spin and valley degeneracy, $k_F = \hbar^{-1}(2mE_F)^{1/2}$ is the Fermi wavevector.

The effects that appear when a magnetic field is switched on are evident already in the Thomas-Fermi approximation, which holds in the long-wavelength limit. The resulting expression (see Ref. 4),

$$\tilde{\varkappa}(\mathbf{k}) = 1 + \frac{2\pi e^2}{\varkappa k}\,\frac{\mathrm{d}n_S}{\mathrm{d}E_F}, \qquad (2.13)$$

indicates that the permittivity oscillates with the filling factor just like the thermodynamic density of states $D_T(E_F) = \mathrm{d}n_S/\mathrm{d}E_F$. In the noninteracting electron approximation the δ-function character of the DS peaks implies that at zero temperature $\tilde{\varkappa}(\mathbf{k})$ goes to infinity for all values of n_S, except for those that correspond to integral filling of Landau levels (at these n_S values screening disappears and $\tilde{\varkappa}(\mathbf{k}) \equiv 0$).

A more accurate calculation of $\tilde{\varkappa}(\mathbf{k})$ requires the calculation of electron gas polarization in the random phase approximation. For a two-dimensional system in a magnetic field no complete solution exists, but in the case of a nonintegral filling factor the more important part of $\tilde{\varkappa}(\mathbf{k})$, related to transitions inside the Nth partially filled level, has been derived by Labbe:[24]

$$\tilde{\varkappa}(\mathbf{k}) = 1 + \frac{e^2}{\varkappa k l_H^2}\,\frac{\nu'(1-\nu')}{T}\,L_N\left(\frac{k^2 l_H^2}{2}\right)\exp\left(-\frac{k^2 l_H^2}{2}\right), \qquad (2.14)$$

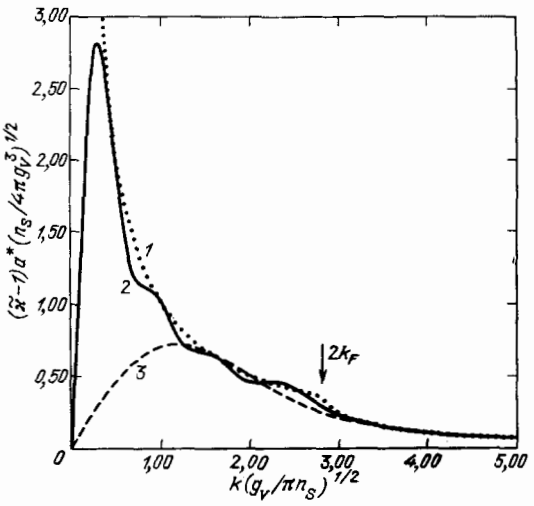

FIG. 1. Permittivity as a function of the wavevector in a two-dimensional (2D) electron system in the absence of a magnetic field (1); and with complete filling of four (2) or one (3) of the lowest Landau levels.

where ν' is counted from the nearest integral value, L_N is a Laguerre polynomial. Note that as $T \to 0$ $\tilde{\varkappa}(\mathbf{k})$ goes to infinity for all $\mathbf{k}$ (in (2.13) this was formally true only for $k \to 0$). In order for (2.14) to hold the resulting self-consistent potential should be small compared to T; at low temperatures electron concentration fluctuations due to screening should be small compared to the mean density of screening carriers $\nu'(1-\nu')/2\pi l_H^2$.

Now let us consider the particular case of linear screening at integral filling factors, when the 2D-system acts like an insulator with respect to the excitation spectrum. The energy gap in the spectrum leads to the suppression of screening when $k \to 0$, but at finite k screening can be quite appreciable because the "dielectric" gap is small.

The calculation of the permittivity $\varkappa(\mathbf{k})$ of a two-dimensional channel in the random phase approximation involves summing the transition matrix elements from every filled level to every empty one. This sum is quickly cut off by the rapid decrease of matrix elements with level separation. In Fig. 1 we show the dimensionless dependence of $\tilde{\varkappa}(\mathbf{k})$ for various numbers of filled levels (up to and including N_F) in an infinitely narrow two-dimensional channel. For comparison we also plot $\tilde{\varkappa}(\mathbf{k})$ for the same channel in the absence of a magnetic field, calculated from (2.12) with $k_F = [2(N_F + 1)]^{1/2} l_H^{-1}$. Clearly the dielectric nature of the screening manifests itself only in the long-wavelength region $kl_H \ll (N_F + 1)^{-1/2}$ where, instead of the $\sim k^{-1}$ divergence that holds in the absence of a magnetic field, we have a linear dependence:

$$\tilde{\varkappa}(\mathbf{k}) = 1 + 2g_V (N_F + 1) \frac{kl_H^2}{a^*}. \qquad (2.15)$$

In the region of wavelengths comparable to the orbit size on the highest filled Landau level $kl_H \ll (N_F + 1)^{-1/2}$, the permittivity is maximized and equals

$$\tilde{\varkappa}(\mathbf{k}) \approx 1 + 2g_V (N_F + 1)^{1/2} \frac{l_H}{a^*}.$$

For shorter wavelengths $\tilde{\varkappa}(\mathbf{k})$ agrees fairly closely with (2.12) (especially at large N_F).

The long-wavelength asymptotic behavior of (2.15) can be easily derived by considering the shift of Larmor orbits caused by the local electric field, as was done in studies of current distribution in the quantum Hall effect.[25]

The decrease in the inhomogenous Landau level broadening due to linear screening depends on the characteristic potential correlation length scale d. Although this decrease disappears in the smooth potential limit $d \gg l_H$, for realistic problem parameters it remains significant. In any case, it is no less important than the other effects obtained in the single-level approximation by expanding in terms of magnetic length. For example, given a Gaussian form of the correlator (2.4) one can expand the level width in terms of the magnetic length as follows:

$$\Gamma_N^2 = \Gamma^2 \left[1 - 2(N_F + 1) \left(\frac{l_H}{d} \right)^2 - 2\pi^{1/2} g_V (N_F + 1) \frac{l_H^2}{da^*} - 12 g_V^2 (N_F + 1)^2 \frac{l_H^4}{(da^*)^2} \right].$$

It is evident that the first term in the expansion, which follows from expression (2.9) for noninteracting electrons, is of the same power in l_H as the second term, which is due to polarization screening (the third term has the same physical origin). But the second term is the leading term in the inverse correlation length d^{-1}. Therefore, screening is fundamentally important even in calculations of broadening caused by weak random potentials. Asymptotic expressions[15] that ignore this fact have limited validity.

Let us estimate the effective screening in a 2D-system at integral filling factors. Linear screening alone suffices only in MIS-structures: because if there is no screening by a conducting electrode even a small concentration of charged impurities near the channel would create a long-range potential with infinite dispersion Γ (see Sec. 2.1). If the dielectric has a thickness $h = 2.0 \cdot 10^{-5}$ cm and contains a charged impurity concentration $n_3 \sim 10^{15}$ cm^{-3}, then the potential dispersion $\Gamma \approx 6$ meV, of the order of the level separation $\hbar\omega_c$ for $H = 10$ T. The dispersion of the screening potential (2.7a) with $\tilde{\varkappa}(\mathbf{k})$ corresponding to the filling of the ground Landau level only $N_F = 0$ (see Fig. 1) is smaller by approximately a factor of two. Thus we can safely rely on the applicability of linear screening, i.e., on the smallness of dispersion Γ compared to $\hbar\omega_c$, for fields $H < 10$ T.

2.4. Nonlinear screening

The fundamental importance of nonlinear effects in the screening of a large-amplitude external potential is due to the fact that it is precisely the nonlinear effects that determine the dependence of the energy spectrum on the filling of Landau levels by carriers. The main nonlinear mechanism is implicit in the fact that the effective number of screening carriers, i.e., carriers free to move in the 2D-plane, itself depends on Landau level broadening. Carriers appear in the tails of the highest filled or the lowest empty level as these tails cross the Fermi level E_F. As the level broadens the number of screening carriers increases, which in turn reduces the level broadening. Consequently the broadening is determined self-consistently and depends on the position of unperturbed levels with respect to the chemical potential.

The most common approach to nonlinear screening springs from Ref. 26 by Ando. It is based on the self-consis-

tent Born approximation (see Sec. 2.2) with corrections due to screening.[27-30] Various random potential models have been considered within this framework, but the thermodynamic density of states has not been studied. When this method is rigorously applied it yields reasonable values for level broadening, although the square-root edges in the density of states may appear as nonanalyticities in calculated dependences of level broadening on the filling factor (this apparently happened in the calculations of Ref. 28). Gudmundsson and Gerhardts[31] developed an interesting, albeit somewhat artificial, method wherein spatial fluctuations of the potential and the electron concentration are replaced by purely statistical ones. This study focused on the thermodynamic density of states, but it furnished only a qualitative illustration of "plateau" formation in $D_T(E_F)$ due to broadening oscillations.

The abovementioned methods required numerical calculations[26-30] whose results were unhelpful in building up a clear physical picture and discerning qualitative dependences. A major advance in the study of nonlinear screening of long-range potentials was accomplished by employing methods developed in the theory of doped semiconductors.[32] These methods were applied to two-dimensional systems by Gergel' and Suris[33] (without a magnetic field), Luryi,[34] Shklovskiĭ and Efros.[35] These studies treated a potential created by Coulomb centers scattered in the plane of the channel,[33,34] or throughout the bulk,[33,35] both for low electron concentrations in the channel[33] and at near-integral filling factors.[34,35] Although the approximations employed in these studies appear to require very strong magnetic fields in real systems (see below), the resulting picture undoubtedly sheds light on the structure of the self-consistent potential and the density of states in strong magnetic fields. We shall describe this picture below, omitting for simplicity the spin and valley degeneracy of the Landau levels.

When the characteristic length scale of the random potential is large compared to the magnetic length l_H, we can speak of the local positions of Landau levels $E_N(r)$ and of their fluctuations in the channel plane that follow the self-consistent potential $\tilde{U}(\mathbf{r})$. The long-range potential shifts the local bottom of the band in the two-dimensional channel together with all the Landau levels

$$E_N(\mathbf{r}) = \tilde{U}(\mathbf{r}) + \left(N + \frac{1}{2}\right)\hbar\omega_c.$$

Let the chemical potential fall between levels N_F and $(N_F + 1)$ in the absence of inhomogeneities, i.e., levels with $N < N_F$ are full and levels with $N > (N_F + 1)$ are empty. Because of fluctuations, the empty $(N_F + 1)$ Landau level can fall below the chemical potential E_F in some places and, conversely, in other places the filled N_F level can climb above E_F. Accordingly, in appropriate regions electrons will appear in the $(N_F + 1)$ level and holes will appear in the N_F level. They create an electrostatic potential that compensates external potential fluctuations and shifts the local position of the appropriate Landau level towards E_F. In the limit of a strong magnetic field the exchange and correlation effects of the Coulomb interaction become unimportant and we have threshold screening. This means that in regions with holes on the N_F level its energy $E_{N_F}(\mathbf{r})$ becomes precisely equal to E_F, whereas in regions where electrons appear on the $(N_F + 1)$ level $E_{(N_F+1)}(\mathbf{r}) = E_F$. As a result the Nth Landau level is "clamped" in the interval:

$$E_F - \hbar\omega_c (N_F - N + 1) \leqslant E_N(\mathbf{r}) \leqslant E_F - \hbar\omega_c (N_F - N). \tag{2.16}$$

The exact form of the density of states $D(E)$ requires numerical computations even in the threshold screening approximation. Nonetheless, some qualitative features can be understood on the basis of graphic dimensional arguments.[35] Below we shall develop a somewhat more general argument, similar in content to Ref. 33. Consider the situation when the concentration n_S is fixed and the filling factor is nearly integral, i.e. the difference $\delta n_S = n_S - [(N_F + 1)/(2\pi l_H^2)] \ll (2\pi l_H^2)^{-1}$. Let us find the position of E_F. First, consider the case of positive δn_S, when the screening carriers are electrons in the $(N_F + 1)$ level and their concentration is δn_S. Take a random potential, described by the correlator Q_k, which we will gradually turn on beginning with its long-wavelength Fourier harmonics up to some k_{max}. At small k_{max} there is complete screening. Screening a plane wave $U(\mathbf{r}) = \exp(i\mathbf{kr})$ requires a change in carrier concentration $\delta n_S(\mathbf{r}) = (\bar{\varkappa}k/2\pi e^2)\exp(i\mathbf{kr})$. Thus, if potential harmonics from $k = 0$ to $k = k_{max}$ are totally screened the characteristic concentration fluctuation is:

$$\delta n_S(k_{max}) \sim \left[\int_0^{k_{max}} Q_k \left(\frac{\bar{\varkappa}k}{2\pi e^2}\right)^2 k \frac{dk}{2\pi}\right]^{1/2}.$$

The screening is ideal if the local electron concentration $n_S(\mathbf{r})$ does not turn to zero anywhere. When k_{max} is small the increase of the concentration $\delta n_S(\mathbf{r})$ is also small and the regions which are fully depeleted by the local decrease in $n_S(\mathbf{r})$ are few. However, as shorter wavelength fluctuations are turned on, the concentrations $\delta n_S(\mathbf{r})$ increase and, at some value $k_{max} = L^{-1}$ determined by the equation

$$\delta n_S^2 \sim \int_0^{L^{-1}} Q_k \left(\frac{\bar{\varkappa}k}{2\pi e^2}\right)^2 k \frac{dk}{2\pi}, \tag{2.17}$$

they become comparable to the mean concentration δn_S. This implies that the screening is markedly nonideal and the distribution $n_S(\mathbf{r})$ of electrons in the plane contains charge-free regions of size L and equally large regions where the electron concentration has been roughly doubled. Harmonics with $k > L^{-1}$ are screened but weakly and, consequently, these harmonics are the ones responsible for level broadening. If we ignore the non-Gaussian nature of the resulting potential, this broadening can be estimated as

$$\Gamma^2 \sim \int_{L^{-1}}^{l_H^{-1}} Q_k k \frac{dk}{(2\pi)^2}. \tag{2.18}$$

The upper bound of the above integral is taken to be the magnetic length, since potential fluctuations of shorter wavelength do not contribute to level broadening (see Sec. 2.2). Expression (2.18) and equation (2.17) determine the characteristic length scale L and amplitude Γ of self-consistent potential fluctuations.

The position of the Fermi level E_F is established by the following considerations. In the absence of impurities it coincides with the partially filled Landau level N_F. Because of self-consistent potential fluctuations of amplitude Γ the Fer-

mi level will move to the fluctuation-induced lower bound of this level $E_{(N_F+1)}(\mathbf{r})$

$$E_F = \hbar\omega_c\left(N_F+\frac{3}{2}\right)-\Gamma, \tag{2.19a}$$

since the electrons will occupy most energetically favorable orbitals. This same argument can be carried out for negative δn_S, when holes are the screening carriers and their concentration is $\delta n_S \ll (2\pi l_H)^{-1}$ in an almost filled level N_F. In this case one obtains the same expressions (2.18), (2.19) for L and Γ, but the chemical potential is now located at the fluctuation-induced upper bound of the $E_{N_F}(\mathbf{r})$ Landau level:

$$E_F = \hbar\omega_c\left(N_F+\frac{1}{2}\right)+\Gamma. \tag{2.19b}$$

The above approach is strictly valid only when the filling factor is not too close to an integer, because it is assumed that Landau level broadening Γ is small compared to inter-level spacing $\hbar\omega_c$ and that the chemical potential is located near the N_F level (for $\delta n_S<0$) or the (N_F+1) level (for $\delta n_S>0$). Generally, screening carriers exist in both levels and their total concentration δn_S enters into (2.17). In cases of integral filling factors $\delta n_S = 0$ and the screening length is determined by (2.18) with level broadening set equal to inter-level spacing. Then expression (2.17) yields the total concentration of screening carriers of both signs.

The expressions listed above illustrate the qualitative dependence of level broadening Γ and Fermi level position E_F on concentration δn_S in a random, long-range potential. Now let us turn to concrete examples of different charged impurity distributions, which requires the substitution of appropriate correlators into equations (2.17) and (2.18). If the potential is produced by charges with a uniform distribution (2.8), integration in (2.18) can be taken to infinity (assuming $l_H \ll L$) and we find

$$L \sim \frac{n_3\delta n_S^{-2}}{4\pi}, \quad \Gamma \sim \frac{e^2 n_3}{2\bar{\varkappa}\delta n_S} \tag{2.20}$$

(given $\Gamma \ll \hbar\omega_c$). As demonstrated in Ref. 35, in the threshold screening limit this case yields a dimensionless universal relation between the chemical potential and the concentration

$$E_F = \hbar\omega_c\left(N_F+1+\Phi\left(\frac{\delta n_S a^*}{n_3 l_H^2}\right)\right), \tag{2.21}$$

where $\Phi(x)$ is a dimensionless, odd function that must be computed numerically. The asymptotic behavior of this function at large values of the argument follows from (2.20)

$$\frac{1}{2}-|\Phi(x)| \sim |x|^{-1}.$$

When the charges are distributed in a plane the situation is more complex. When the correlator (2.6) is substituted into the integral (2.18) for level broadening, the integral diverges logarithmically at the upper bound and the magnetic length l_H appears explicitly in the result:

$$L \sim \left(\frac{n_2}{4\pi}\right)^{1/2}\delta n_S^{-1}, \quad \Gamma \sim \frac{e^2}{\bar{\varkappa}}\left(2\pi n_2 \ln\frac{n_2^{1/2}}{\delta n_S l_H}\right)^{1/2}.$$

The position of the chemical potential is established by (2.19). Obviously the dependence of E_F on n_S is no longer dimensionless. The thermodynamic density of states, which follows from (2.20) or (2.21), exhibits a power-law divergence near each Landau level

$$D_T(E_F) \sim \frac{e^2 n_3}{\bar{\varkappa}(\Delta E_F)^2},$$

where ΔE_F is the separation between E_F and the nearest Landau level. The thermodynamic DS is minimized

$$D_T(E_F) \sim \frac{e^2 n_3}{\bar{\varkappa}(\hbar\omega_c)^2} \sim \frac{n_3 l_H^2}{a^*\hbar\omega_c}$$

when E_F falls half-way between two Landau levels, i.e. when $\Delta E_F \approx \hbar\omega_c/2$. When the impurities are distributed in two dimensions, $D_T(E_F)$ falls off exponentially as E_F moves further from the Landau level,

$$D_T(E_F) \sim \frac{\Delta E_F \bar{\varkappa}^2}{e^4 l_H n_2^{1/2}}\exp\left(-\frac{\Delta E_F^2\bar{\varkappa}^2}{n_2 e^4}\right),$$

When E_F reaches half-way between levels $D_T(E_F)$ becomes exponentially small:[35]

$$D_T(E_F) \sim \frac{(a^*)^2}{l_H^5\hbar\omega_c n_2^{1/2}}\exp\left(-\frac{(a^*)^2}{n_2 l_H^4}\right). \tag{2.22}$$

Let us analyze the validity of our estimates in the case of a bulk impurity distribution. In addition to the usual constraint that the electron-electron interaction be weak, $l_H/a^* \ll 1$, several other conditions apply.

1. The screening length L must be large compared to:

a) the separation between impurities, $n_3 L^3 \gg 1$ (so the potential can be treated as Gaussian),

b) the magnetic length l_H (more precisely, the orbit size on the levels contributing to the screening).

2. The concentration of screening carriers in (2.17) must be small compared to:

a) total number of orbitals in the level, $\delta n_S \ll (2\pi l_H)^{-1}$

b) the characteristic concentration at which the correlational energy shifts become comparable to level broadening, $(e^2/\bar{\varkappa})\delta n_S^{1/2} \ll \Gamma$.

The theory is best suited to real systems when the filling is integral, E_F is located precisely half-way between levels, and the broadening reaches its maximum value $\Gamma \sim \hbar\omega_c$. In this case all the constraints reduce to a restriction on the magnetic field intensity. In principle, the most stringent requirement is 2.a) which can be rewritten using (2.20) as

$$l_H^4 n_3 \ll a^*. \tag{2.23}$$

It is more difficult to estimate the constraints in the flat Impurity distribution problem, but up to a logarithmic coefficient it probably suffices that the exponent in (2.22) be large compared to unity:

$$l_H^4 n_2 \ll (a^*)^2. \tag{2.24}$$

Since the numerical coefficients in these estimates are unknown, inequalities (2.23), (2.24) should not be taken as quantitative criteria, but rather as qualitative lower bounds on the magnetic field intensity that would render the threshold screening hypothesis valid, at least for integral filling.

The presence of a conducting electrode imposes an additional constraint that the screening length be small compared to the distance to the electrode $L \ll h$, which places an upper bound on the magnetic field. If this constraint is violated significant screening of the random potential by the electrode will follow. In the opposite limit $L \gg h$, the two-dimensional channel does not participate in the screening at all.

To date, the rather interesting question of the shape of the single-particle DS peaks in the case of nonlinear screening has not been examined in detail. Self-consisent calculations[26-30] are entirely inapplicable since they ivariably yield a semielliptical peak shape. Qualitative arguments[34] within the threshold screening model indicate that each Landau level $E_N(\mathbf{r})$ has a greater probability of being located at the edges of iterval (2.16), rather than in its original position in the absence of a random potential. A better understanding will require numerical modelling that approximates the real situation. Currently, all experimental data fit into the traditional representation of the single-particle density of states by a collection of bell-shaped peaks corresponding to broadened Landau levels.

3. EXPERIMENTAL METHODS OF STUDYING THE THERMODYNAMIC DENSITY OF STATES

Practically all methods that purport to measure the thermodynamic DS are based on the oscillatory response of the total energy (E), chemical potential (E_F), or magnetization (M) of a 2D-electron system to variation in the magnetic field. Consequently, let us examine the oscillation of these quantities in the simplest case: an ideal system of noninteracting 2D-electrons at $T=0$ and $n_S = \text{const}$.[36] As we have seen already, in this ideal system the energy spectrum consists of a collection of δ-functions separated by cyclotron energy gaps (for now we shall neglect spin and the nonequivalence of different electron valleys for simplicity). If the magnetic field intensity is so great that the 2D-electron concentration n_S is smaller than the Landau level degeneracy H/eh (i.e. $\nu < 1$), all electrons will be found in the ground state on the lowest level. Then the total energy, chemical potential, and magnetic moment of the system are $0 < \nu < 1$:

$$E = \frac{1}{2}\hbar\omega_c S n_S,$$
$$M = -\frac{dE}{dH} = -\frac{1}{2}\frac{e\hbar}{m} S n_S, \qquad (3.1)$$
$$E_F = \frac{1}{S}\frac{dE}{dn_S} = \frac{1}{2}\hbar\omega_c;$$

where S is the area of the 2D-system and m is the effective electron mass.

If the field intensity is reduced with n_S held fixed (i.e., ν increases) then, with $1 < \nu < 2$, part of the electrons will fill the lowest Landau level and the rest will be found in the first excited level with $N = 1$.

$1 < \nu < 2$:

$$E = S\frac{eH}{h}\frac{\hbar\omega_c}{2} + \frac{3}{2}\hbar\omega_c S\left(n_S - \frac{eH}{h}\right)$$
$$= \frac{3}{2}\hbar\omega_c S n_S - \hbar\omega_c S\frac{eH}{h},$$
$$M = -\frac{1}{2} S n_S \frac{\hbar e}{m}\left(3 - \frac{4}{\nu}\right), \qquad (3.2)$$
$$E_F = \frac{3}{2}\hbar\omega_c.$$

In the general case of $k < \nu < (k+1)$ (k an integer) it is easy to show that:

$$E = (2k+1) S n_S \frac{\hbar\omega_c}{2} - k(k+1)\frac{\hbar\omega_c}{2} S\frac{eH}{h},$$
$$M = -\frac{1}{2} S n_S \frac{\hbar e}{m}[(2k+1) - 2k(k+1)\nu^{-1}], \qquad (3.3)$$
$$E_F = \frac{1}{2}(2k+1)\hbar\omega_c.$$

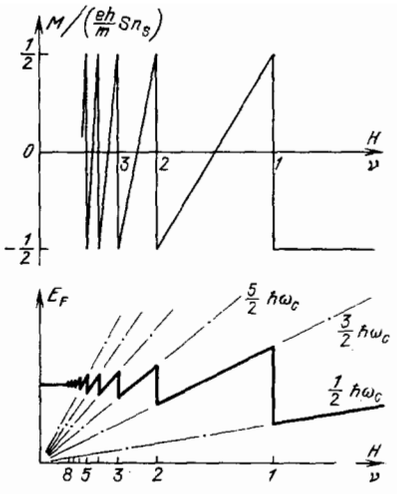

FIG. 2. Schematic picture of the oscillatory behavior of magnetization M and chemical potential E_F of an ideal 2D-electron gas at a constant concentration n_S in a magnetic field, $T = 0$.

The qualitative dependences $M(H)$ and $E_F(H)$ that result from these formulas are illustrated in Fig. 2. Evidently, at integral values of ν both the chemical potential and the magnetization jump sharply. The formulas clearly indicate that the E_F jumps correspond to the energy gap $\hbar\omega_c$ and the magnetic moment changes from $-(1/2)Sn_S e\hbar/m$ to the opposite value $(1/2)Sn_S e\hbar/m$. Certainly in a real 2D-system imperfections and a finite temperature ($T \neq 0$) should wash out these jumps and decrease their amplitude. Moreover, the spin and intervalley splittings that are present in the energy spectra of real 2D-electron systems should produce additional chemical potential jumps. At ν values when both Landau spin sublevels are completely filled the magnetization jumps by $Sn_S e\hbar/m$, while at ν values when one spin sublevel

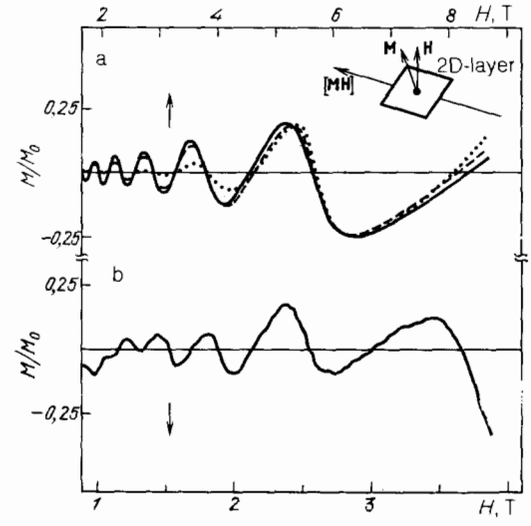

FIG. 3. Oscillations in the normalized magnetization of 2D-electrons in a GaAs-AlGaAs heterostructure in a magnetic field.[8] a—Heterostructure with 140 identical quantum wells, 2D-electron concentration in the wells $n_S = 5.4\times10^{11}$ cm^{-2}, electron mobility $\mu = 8\times10^4$ cm^2/V·s; b—Single heterojunction, $n_S = 3.7\times10^{11}$ cm^{-2}, $\mu = 2.85\times10^5$ cm^2/V·s; inset shows the experimental geometry; dashed and dotted lines are fits calculated by assuming Gaussian DS peaks on Landau levels with different broadening estimates.

is filled and the other empty M jumps by $Sn_S g_e e\hbar/m_0$ where g_e is the 2D-electron g-factor and m_0 is the free electron mass. These oscillations have been observed in magnetization M[5] and contact potential V_c[37] measurements. In experiments measuring the heat capacity c_T[6] and electronical capacitance C_e[38] of 2D-electron systems the observed structures were also due to chemical potential oscillations in a magnetic field. We shall now consider individually all of these experimental methods which are used to determine the thermodynamic DS of 2D-electrons in a magnetic field.

3.1. Magnetization oscillations

Magnetization measurements in a 2D-electron system were first reported in Ref. 5. In these experiments the samples were mounted on a thin fiber held perpendicular both to the magnetic field and to the normal to the 2D-layer plane. The magnetic field was tilted by a small angle from the normal to the 2D-layer in which direction the orbital magnetic moments of 2D-electrons would point. The torque under such a condition is determined by $\mathbf{M}\times\mathbf{H}$ and therefore depends on the total magnetization of the 2D-electron system. The oscillating part of this magnetization was measured using a highly sensitive torque magnetometer. Detailed descriptions of the instruments used in this technique and of the differential capacitance method of measuring magnetization deflection angles in a slowly swept magnetic field are available in Refs. 5, 39, 40.

Different 2D-electron systems were studied in these experiments: a GaAs-AlGaAs superlattice containing some 100 quantum wells with 2D-electrons (of fairly low mobility $\sim 5\times 10^4$ cm^2/V·s), as well as a single GaAs-AlGaAs heterojunction with high mobility. In both cases, instead of abrupt magnetization jumps at integral filling factors, the authors measured a fairly smooth variation of magnetization with H (Fig. 3). The amplitude of M oscillations was significantly smaller (by almost a factor of five) than the theoretical value $M_0 = n_S S\hbar e/m$ (see (3.3)). These observations imply that there is great broadening and overlap of the Landau levels in QHE conditions, inasmuch as even the high field ($\mu H \gg 1$) density of states does not become small between Landau levels but rather makes up a significant fraction of the zero-field two-dimensional DS: $D_0 = m/\pi\hbar^2$.

In order to calculate the DS the experimental $M_e(H)$ dependence was compared with the theoretical $M_t(H)$ counterpart obtained by differentiating the expression

$$E = \int_0^\infty \varepsilon D(\varepsilon, \Gamma) f(\varepsilon, E_F, T)\, d\varepsilon, \qquad (3.4)$$

with respect to the magnetic field (where $f(\varepsilon,E_F,T)$ is the Fermi distribution function).

In this expression each DS peak was described by the Gaussian

$$D(\varepsilon, \Gamma) = \frac{eH}{h}\sum_j D_j(\varepsilon),$$

$$D_j(\varepsilon) = \pi^{-1/2}\Gamma^{-1}\exp\left[-\frac{(\varepsilon - E_j)^2}{2\Gamma^2}\right] \qquad (3.5)$$

(E_j are the energies of unbroadened Landau levels). The parameter Γ was taken to depend on the magnetic field. The best fit to the data was obtained with $\Gamma = AH^{1/2}$, where the constant A depends (rather weakly) on the quality of the structure and decreases with increasing μ.

In summary, we note that magnetization measurements in 2D-systems did not succeed in directly measuring the density of states. The weakest link in this method is the assumption that the fitting parameter Γ depends monotonically on H and is independent of the filling factor. It follows immediately from experimental and theoretical arguments[26,35] that this assumption is invalid and hence the quantitative DS descriptions presented in Refs. 5, 39, 40 prove rather crude. We emphasize, on the other hand, that these experiments furnished some of the first indications that Landau levels overlap strongly under QHE conditions and that the DS in the gaps is significant even in a very strong magnetic field (i.e., when $\mu H \gg 1$).

3.2. Contact potential and gate current oscillations

The contact potential method, employed in Refs. 37, 41-43 to study the 2D-electron density of states, is essentially identical to the classic Kelvin method used to measure the electronic work function of a material. This experimental technique measures the difference in contact potentials V_c of the 2D-electron channel (with constant electron concentration) and the metallic electrode as a function of magnetic field. If the magnetic field has no effect on the gate, whereas the chemical potential of 2D-electrons oscillates with magnetic field according to (3.3), then the measured difference in V_c (under conditions of thermodynamic equilibrium necessary to maintain a constant electrochemical potential) should reflect the Fermi level oscillations of a 2D-electron system in a magnetic field.

We note that the idea of applying the contact potential difference method to study the electronic energy spectrum in a magnetic field was proposed in 1986 in Refs. 44 and 45. Experimental results on metals (Be), however, proved negative: no contact potential oscillations due to chemical potential changes in a magnetic field were observed, even though the measurement sensitivity far exceeded the expected magnitude of V_c oscillations.[46] This negative result was explained in Ref. 47 by noting that in this case electrons determine the compressibility of a metal and hence the contact potential oscillations cannot follow chemical potential oscillations, as they are completely compensated by the magnetostriction effect. It might have been expected that in semimetals, where the bulk electron concentration is lower by 3-4 orders of magnitude compared to ordinary metals, magnetostriction effects would be weak and V_c oscillations would appear. Yet Ref. 47 established that even in semimetals contact potential oscillations are fully compensated. Consequently, the potential oscillations between the metallic gate and the 2D-channel in silicon MIS-structures measured in Ref. 37 were probably the first experimentally observed contact potential oscillations of a metallic system in a magnetic field. In addition to silicon MIS-structures, V_c oscillations have been observed in GaAs-AlGaAs heterojunctions.[48,49]

In experiments on Si MIS-structures[37,41-43] V_c variation was measured using an electrometer with a large input impedance ($\sim 10^{14}\ \Omega$) to make sure that during the period of a $V_c(H)$ oscillation the charge on the MIS-structure did not change by more than 0.1%. The dependence

$$V_c(H)\,|_{n_S=\text{const}}$$

exhibited contact potential jumps, which were most pronounced at integral filling factors $\nu = 4, 8, 12 \ldots$ corresponding to complete Landau level occupation. Since in the ideal case the magnitude of the chemical potential jump at $\nu = 4, 8, 12 \ldots$ approximately equals $\hbar\omega_c$ (see Fig. 2) the oscillation amplitude ΔV_c should reach $\hbar\omega_c/e$. Yet the experimentally measured ΔV_c were reduced by almost a factor of five, indicating singificant Landau level broadening compared to the ideal case. The energy spectrum parameters of 2D-electrons were extracted by Pudalov and co-workers[41] from the best fit of the measured dependence $\Delta V_c(H)$ to the function $E_F(H)/e$ obtained by numerically solving the equation:

$$n_S = \frac{eH}{h} \sum_j \int_0^\infty D_j(\varepsilon, E_F) \left(1 + \exp\frac{\varepsilon - E_F(H)}{kT}\right)^{-1} d\varepsilon. \tag{3.6}$$

This equation, derived from the condition of constant 2D-electron concentration in a magnetic field, contains the functions $D_j(\varepsilon)$ which describe the energy distribution of the density of states on the Landau levels. In fact, these functions make it possible to study the DS by the contact potential difference method. It should be noted, however, that several assumptions and fitting parameters are required if this method is to yield the density of states. These include:

1. The equality $\Delta V_c(H) \equiv \Delta E_F(H)$, even though it may be violated by compensating effects related, for example, to magnetostriction.[47]

2. The energy distribution of the density of states on two adjacent Landau levels is assumed to follow Gaussians of width Γ, which is a fitting parameter assumed constant for adjacent sublevels.

3. Another fitting parameter is the energy gap $\Delta\nu$, corresponding to the filling factor ν.

4. Since in some ranges of magnetic field the experimental dependence $\Delta V_c(H)$ is measured under conditions of changing ν, the fitting parameters $\Delta\nu$ and Γ are not constants, as follows from Ref. 8 and the conclusions of Ref. 41, but instead could change sharply according to unknown dependences $\Delta\nu(H)$ and $\Gamma(H)$.

These difficulties make the quantitative results of contact potential measurements less reliable, but it should be noted that this method succeeded in discoverning the enhancement of intervalley and spin splittings.[41]

Experiments measuring the contact potential difference are closely related to the gate current oscillation technique of studying the DS, wherein the current flowing through the 2D-channel-gate raise circuit is measured in a ramped magnetic field. This technique was proposed in Ref. 50 to study the DS in GaAs-AlGaAs heterstructures. The chemical potential of 2D-electrons oscillates in a changing magnetic field, resulting in contact potential difference oscillations and charge transfer in the gate-2D-channel circuit. This charge transfer should follow the contact potential difference oscillations. The quantity of charge can be determined by measuring the current through the gate-2D-channel circuit closed with a load resistance. The current then equals

$$I(H) = Se\frac{dn_S}{dt} = Se\frac{dn_S}{dH}\frac{dH}{dt}, \tag{3.7}$$

where S is the area of the 2D-electron channel, dH/dt is the magnetic field sweep rate. It follows immediately from (3.7) that measurements of the gate current $I(H)$ also contain information on the density of states.

3.3. Electronic heat capacity oscillations

Another method of obtaining the 2D-electron density of states in a quantizing transverse magnetic field is based on measuring the electronic heat capacity, which is defined by

$$c_T = \frac{dE}{dT} = \frac{d}{dT}\int_0^\infty \varepsilon D(\varepsilon) f(\varepsilon, E_F)\, d\varepsilon, \tag{3.8}$$

where E is the internal energy of the electronic system. As the temperature changes electrons are redistributed in the vicinity of the Fermi surface. The electronic heat capacity is therefore proportional to the DS at the Fermi level, which follows from equation (3.8). It should be emphasized that both extended and localized electron states contribute to the heat capacity.

The heat capacity of 2D-electron systems was calculated in Ref. 51, which implicitly assumed a single-particle DS on Landau levels and a Gaussian distribution of $D(E)$. That paper analyzed the intra-level and inter-level contributions to the heat capacity. If several Landau levels contribute, the electronic heat capacity oscillates with filling factor, so that $c_T(\nu)$ is maximized at integral ν and minimized at half-integral ν. These peaks appear only when $kT \sim \hbar\omega_c$ (i.e., when temperature is fairly high compared to the gaps in the energy spectrum).

Electronic contribution to the heat capacity is much weaker than the phonon term. This posed the main problem in experiments devoted to measuring 2D-electron heat capacity oscillations produced by varying the quantizing transverse magnetic field. The difficulty was overcome, however, by studying multilayer heterostructures consisting of large numbers of identical quantum wells containing the 2D-electron gas. Thus Refs. 5, 50 employed a GaAs-AlGaAs heterostructure consisting of about 100 quantum wells (the total number of 2D-electrons was of the order of 10^{13}). Electronic heat capacity measurements were carried out by the standard heat pulse technique, wherein the system is heated adiabatically. The experimental details are described in Refs. 6, 52.

Figure 4 illustrates the temperature oscillations produced by changes in the magnetic field. Measurements were carried out on a multiquantum well heterostructure at 1.5 K.[52] Temperature changes were obtained from the resistance of a Au-Ge temperature detector (y-axis in Fig. 4) with the resistance variation ΔR proportional to temperature variation ΔT of the sample.

Temperature oscillation peaks produced by a ramped magnetic field correlate precisely with minima of Shubnikov–de Haas oscillations in magnetoconductance $\sigma_{xx}(H)$ and the plateaus in the Hall resistance $\rho_{xy}(H)$ in the same structure. Such a strong correlation in the oscillatory behavior of temperature and magnetotransport coefficients furnishes convincing evidence that the experimentally observed temperature oscillations are due to the electronic heat capacity.

The next step is to extract the density of states from the measured oscillatory behavior of temperature field dependence $\Delta T(H)$ caused by oscillations in the electronic heat capacity. To this end one computes the oscillating behavior

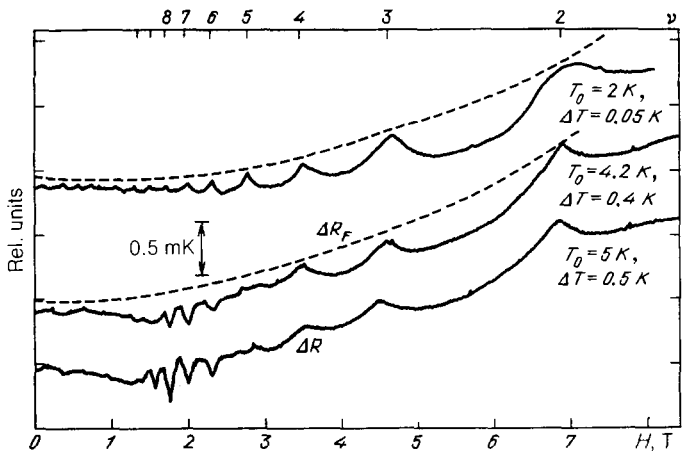

FIG. 4. Electronic temperature oscillations of a 2D-electron gas in a 94 layer GaAsAlGaAs heterostructure as a function of magnetic field.[6] A heat pulse increases the sample temperature by ΔT. The dashed line indicates the increase in lattice temperature.

of electronic heat capacity $c_T^{el}(H)$ (Fig. 5). The computation proceeds from some assumptions on the DS shape at the Landau levels, DS peak width Γ, and the constant DS background D under the peaks (Γ and D are fitting parameters). If an adiabatic heat pulse transfers an amount of heat ΔQ to the sample, then the electronic heat capacity is related to the resulting temperature change ΔT according to following formula:

$$c_T^{el}(T, H, \Gamma) = \frac{\Delta Q}{\Delta T} - \frac{1}{4}\frac{\alpha}{\Delta T}[(T+\Delta T)^4 - T^4], \qquad (3.9)$$

where the lattice heat capacity $c_T^{lat} = \alpha T^3$ and it is assumed that $c_T^{el}(T+\Delta T) \sim c_T^{el}(T)$. The best fit of experimental data to calculated oscillations is obtained when the DS peaks at the Landau levels have width $\Gamma \sim H^{1/2}$ and there is a finite background DS in the spectrum gaps (see Fig. 5). Consequently this method does not directly measure the DS, but rather employs several fitting parameters and apriori assumptions on the shape of DS peaks at Landau levels, as well as assuming a constant DS background of unexplained origin.

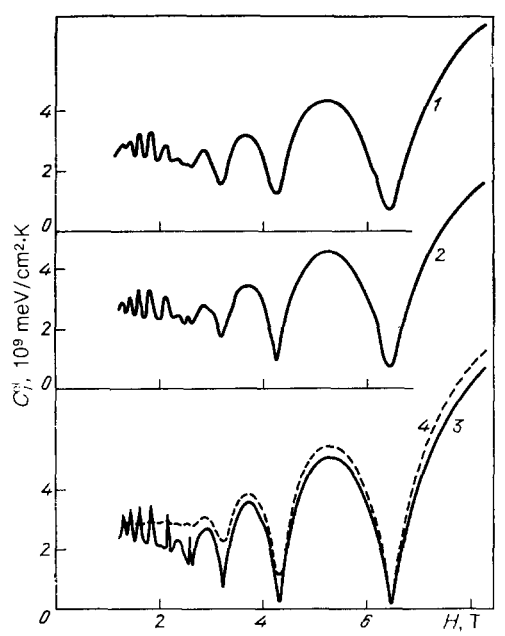

FIG. 5. Electronic heat capacity oscillations calculated from the oscillating electronic temperature dependence shown in Fig. 4.[6] Curve 1—experiment; 2–4—calculations with $\Gamma = 0.6$ meV$\cdot H^{1/2}$, $\Gamma = 0.75$ meV, and $\Gamma = 1.5$ meV respectively.

3.4. Magnetocapacitance oscillations

The capacitance of a metal-insulator-semiconductor (MIS) system does not depend solely on the insulator thickness (h) and the 2D-channel thickness, but also on the electronic density of states.[53] Indeed, if a gate potential variation δV_g induces a δn_S variation in the 2D-electron concentration, then it follows from the constancy of the electrochemical potential in thermodynamic equilibrium that $e\delta V_g = \delta E_F$, where δE_F is the variation of the 2D-electron chemical potential that corresponds to δn_S. We thus obtain the following expression for the magnetocapacitance:

$$C_e = \frac{dq}{dV_g} = Se\frac{\delta n_S}{\delta E_F/e} = Se^2\frac{dn_S}{dE_F} = Se^2 D_T(E_F).$$

Consequently the full inverse capacitance contains three terms:

$$C_e^{-1} = \frac{h}{S\varkappa_0\varkappa_d} + \frac{\gamma z_0}{S\varkappa_0\varkappa_S} + (Se^2 D_T(E_F))^{-1}, \qquad (3.10)$$

where $\varkappa_0$, $\varkappa_d$, $\varkappa_S$, are the vacuum, dielectric (insulator), and semiconductor permittivities respectively; S is the area of the system, D_T is the thermodynamic 2D-electron density of states; and γ is a numerical coefficient in the range of 0.5–0.7.[53] Significantly, the first two terms remain constant in a changing magnetic field and, consequently, capacitance variation with magnetic field is directly related to changes with H in the density of states at the Fermi level. It should be noted that the typical value of the third term in (3.10) at $H = 0$ comprises only $\sim 10^{-3}$ of the first term and hence measurements require great precision in a bridge capacitance scheme,[38,54] wherein one accounts for the phase shifts and frequency dependence of potential variation that accompany changes in the capacitance. The magnetocapacitance method fails at integral Landau level filling at low temperatures and high magnetic fields (i.e., under QHE conditions). The point is that in the quantum Hall effect regime the diagonal conductivity σ_{xx} of a 2D-electron system becomes exponentially small and the voltage signal measured in the bridge scheme ceases to follow capacitance variation and reflects σ_{xx} instead. If the magnetocapacitance method is to measure the pure capacitance signal the following condition must hold

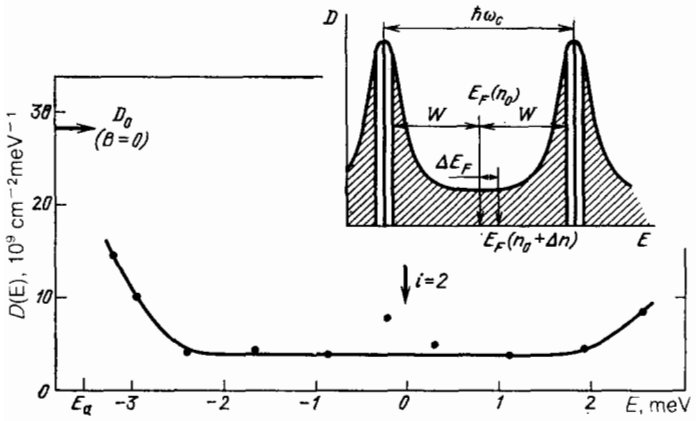

FIG. 6. Density of states as a function of energy obtained from measurements of thermally activated conductance.[7] Measurements done on a GaAs-AlGaAs heterostructure, 2D-electron mobility in the channel $\mu = 1.9\times10^8$ cm^2/V·s. Schematic energy distribution of the single-particle DS corresponding to nearly integral filling factors is shown in the inset. Regions of localized states are shaded.

$$\sigma_{xx} \gg \frac{\omega (C_e^0)^2}{\Delta C_e}, \tag{3.11}$$

where C_e^0 is the field-independent capacitance determined by the first two terms in (3.10), ΔC_e is the capacitance variation due to changes in D_T (third term in (3.10)). The constraint (3.11) turns out to be quite rigorous and makes it practically impossible to determine D_T in the QHE regime. Indeed, if the experimental parameters are $C_e^0 \sim 10^{-9}$ F; $\Delta C_e \sim 10^{-12}$ F; $\omega \sim 10^2$ Hz, then (3.11) requires $\sigma_{xx}^{-1} \ll 10^2$ Ω, whereas in the QHE regime at $T = 2$ K, $H = 8$ T, $\sigma_{xx}^{-1} \geqslant 10^9$–$10^{13}$ Ω. This estimate clearly indicates that inequality (3.11) may only be satisfied far from the QHE regime. The difficulty with measuring the absolute value of the capacitance in the QHE regime also results from the very small "flow-over" length[57] $L_f = (\sigma_{xx} S/\omega C_e)^{1/2}$, which implies that only a fraction of the area of the 2D-electron system (near the source and sink contacts) is probed. Hence a smaller effective area $S^* < S$ should enter into (3.10) and a strong reduction in the measured capacitance in the QHE regime may reflect a smaller S^*, rather than a smaller D_T. There should also be no phase shift in ΔC_e measurements, since conductance through the effective area S^* will be markedly larger than $\sigma_{xx}^{\square}$ (where $\sigma_{xx}^{\square}$ is the conductance of the 2D-electron system per unit area).

The first magnetocapacitance measurements, reported in Ref. 38, attempted to determine D_T between Landau levels at integral ν in a GaAs-AlGaAs heterostructure. At $T \approx 1.3$ K, however, a purely capacitive signal could only be measured with $H < 1.6$ T. In Ref. 54 the authors applied the magnetocapacitance method at half-integral ν, where $\sigma_{xx}^{-1} \sim h/e^2 \sim 10^2$ Ω and found that the Landau level width Γ, determined from the magnetocapacitance values at half-integral ν, varied as $H^{1/2}$, in agreement with the short-range scatterer theory,[23] and depended on the 2D-electron mobility, also in agreement with this theory.

In all, the magnetocapacitance method proved very effective in measuring the 2D-electron density of states precisely on the Landau levels (half-integral ν). In the more interesting quantum Hall effect regime (integral ν) this method appears to encounter insurmountable difficulties.

3.5. Thermally activated magnetoconductance

The notion of determining the 2D-electron density of states from thermally activated magnetoconductance data[7] springs from the assumption that the electronic states in the gaps between Landau levels are localized, while extended states are concentrated in narrow regions near the Landau levels. Taking this assumption as valid, whenever each Landau sublevel becomes fully occupied (i.e., when $n_S = n_S^0 = veH/H$, ν an integer), the Fermi level falls into an energy gap (half-way between Landau levels; see Fig. 6, inset). The magnetoconductance σ_{xx} then falls to its minimum σ_{xx} min and differs from zero (if the temperature is not too low) because of thermal activation of electrons and holes from the Fermi level into the extended states:

$$\sigma_{xx}^{\min} \sim \exp\left(-\frac{W}{kT}\right), \tag{3.12}$$

where W is the activation energy equal to half the energy gap. If the concentration n_S changes from n_S^0 by a quantity Δn_S, the Fermi level shifts by ΔE_F from the midpoint of the energy gap towards one of the Landau levels, which reduces the activation energy by ΔE_F. In this manner, by following the changes in activation energy induced by variation of n_S about n_S^0 one can establish the dependence of ΔE_F on Δn_S and by differentiating obtain the 2D-electron density of states in the energy gaps of the spectrum (see Fig. 6).

Significantly, the thermally activated magnetoconductance method can only hope to determine correctly the quantity $D_T(E_F) = dn_S/dE_F$ in the narrow range near integral filling factors (i.e., in the QHE regime; the thermally activated conductance and magnetocapacitance methods are thus complementary). Precisely in this region, as was shown in Ref. 58, both the electron $\sigma_{xx}^e \sim \exp[-(W - \Delta E_F)/kT)$ and hole $\sigma_{xx}^h \sim \exp[-(W + \Delta E_F)/kT)$ contributions to the magnetoconductance should be considered. Consequently the temperature dependence of magnetoconductance is described by the equation[58]

$$\sigma_{xx}(\Delta n_S) \sim \exp\left(-\frac{W}{kT}\right) \operatorname{ch}\frac{\Delta E_F}{kT}. \tag{3.13}$$

Only then does the differentiation of $\Delta E_F(\Delta n_S)$, obtained from (3.13), yield the correct density of states D_T exactly at the midpoint of the energy gap.

An analysis of thermally activated magnetoconductance led to the following conclusions:[7,58,59]

1) the density of states at the midpoint of the energy gap depends weakly on energy;

2) the quantity D_T is not exponentially small in the energy gaps, but rather makes up an appreciable fraction of D_0 (see Fig. 6) and decreases slowly with increasing μ and H.

The major weaknesses of the thermally activated magnetoconductance method are:

1) the assumption that the density of states $D(E)$ does not depend on Δn_S and T;

2) the assumption that the mobility threshold that separates localized states from extended ones does not change with Δn_S;

3) the method is only valid in a fairly narrow temperature range;

4) in the QHE regime the measured current is strongly inhomogenous (filament formations) and hence the measured density of states may characterize only that part of the 2D-electron system that carries the current.

Nonetheless, it should be noted that the thermally activated magnetoconductance method was the first one used to establish that the 2D-electron density of states in a strong magnetic field is non-exponentially small between Landau levels.[60]

3.6. Other methods

In addition to the discussed methods of experimentally investigating the 2D-electron density of states in a transverse magnetic field, several other techniques addressing the same problem should be mentioned. Shashkin and co-workers[61] employed a method based on the nonlinear characteristics of silicon MIS-structures. Although physically equivalent to the thermally activated magnetoconductance method, this experiment had the advantage of recording the current distribution in the MIS-structure in addition to probing the density of states. Another promising method is the study of resonant tunneling of charge carriers through a thin insulating layer in silicon MIS-structures.[62] Also, cyclotron resonance experiments are of considerable interest.[63,64] A recent advance in that area consisted of observing oscillations in the broadening of cyclotron resonance lines that varied with the filling factor, recorded in an experiment with a fixed filling factor and a swept far-infrared radiation frequency.

4. THE SPECTROSCOPIC METHOD OF STUDYING THE SINGLE-PARTICLE DENSITY OF STATES

Now let us turn to the spectroscopic method of determining the DS of 2D-electrons in a transverse magnetic field. This method is based on recording the luminescence spectra of radiative recombination of two-dimensional electrons with nonequilibrium photoexcited holes. We shall take the Si (001) MIS-structure as an example.[8,66,67] Importantly, this method measures the energy distribution D(E) of a single-particle DS at fixed Landau level filling, whereas the methods described in the preceeding section (see Sec. 3) probed the thermodynamic density of states $D_T(E_F) \equiv dn_S/dE_F$. If electron-electron interaction and random potential screening are taken into account $D(E_F) \neq dn_S/dE_F$. The spectroscopic method makes it possible to followthe redistribution of single-particle DS as the filling of quantum states changes due to screening of the long-range random potential components. Not only does the spectroscopic method furnish an effective tool of studying the fine structure of the Landau levels—spin and valley-orbital splitting, but it provides a means of studying the random potential directly and evaluating its amplitude and range.

4.1. Radiative recombination of 2D-electrons in silicon MIS-structures

The inversion space-charge layer in silicon MIS-structures is the traditional quasi-two-dimensional electron gas system whose properties have been studied most thoroughly. In such structures the Si crystal is covered with a planar, thin (10^{-5} cm) SiO_2 dielectric film. A metallic electrode (gate) is then deposited on top of the dielectric (Fig. 7). The bias V_g applied between the gate and the Si-SiO_2 interface creates a uniform electric field in the dielectric and a potential well in the Si at the interface. The potential well, which contains space-charge, is bounded on the dielecric side by a high potential barrier (~ 2 eV) and has a nearly triangular shape. In equilibirium at sufficiently large V_g the bottom of the well falls below the chemical potential in the bulk of the crystal. Then a thin near-surface layer ($\sim$30-50 Å) is filled with electrons, that is carriers of the opposite sign with respect to the majority carriers in the bulk (holes). Consequently, an inversion space-charge layer forms at the p-Si surface at $V_g > 0$. The channel is filled with carriers either via the source and sink electrodes or by illumination. A depletion layer

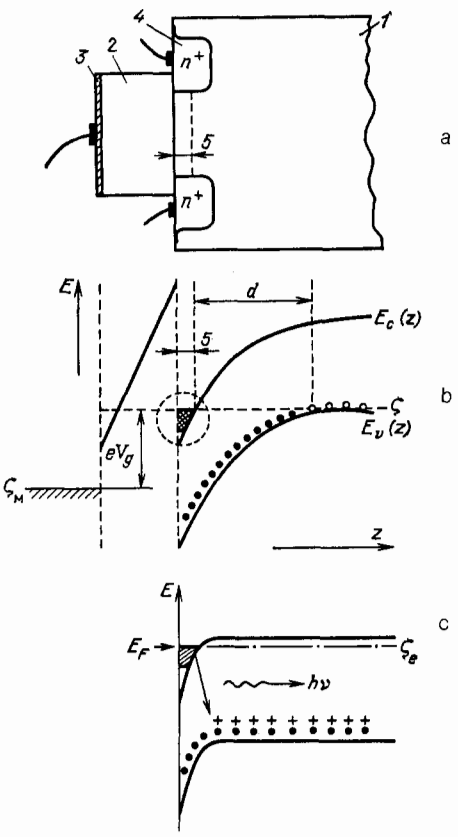

FIG. 7. MIS-structure: schematic cross-section and band-bending diagrams near the oxide-semiconductor interface. a—Schematic crosssection: 1—p-type semiconductor; 2—oxide (dielectric); 3—metallic electrode (gate); 4—low-resistance electrodes (source-sink); 5—inversion layer. b—Energy band diagram in the absence of photoexcitation: E_c and E_v—bottom of the conduction band and top of the valence band in the semiconductor, bottom of the conduction band in the oxide is shown to the left of the channel; ζ—Fermi level in the semiconductor; ζ_m—Fermi level in the metal; V_g—gate potential; L_d—depletion layer width; points—ionized acceptors; crosses—holes on acceptors; shaded region denotes degenerate electron gas. c—Energy band diagram with photoexcitation: ζ_e—quasi-Fermi level of the electrons; $h\nu$—recombination photon energy.

separates the inversion layer from the bulk; since no carriers are present in this layer it acts like an insulator. The depletion layer contains small ionized impurities of the same sign as the carriers in the channel. At low V_g the external electric field is screened only by the depletion layer of thickness $L_D = n_d/N_A \sim 1\ \mu m$ (n_d is the surface charge density in the depletion region, N_A is the bulk acceptor concentration). When the band bending (see Fig. 7) becomes comparable to the bandgap E_g, creating the 2D-channel, increasing V_g further does not alter the charge distribution in the depletion region. The resulting charge and field distribution near the $Si\text{-}SiO_2$ interface can be reconstructed from an analysis of Shubnikov–de Haas magnetoconductance oscillations.[67]

If a steady state photoexcitation generates nonequilibrium electron-hole pairs near the $Si\text{-}SiO_2$ interface, the charge and field distribution changes dramatically (see Fig. 7,c). First, in the case of photoexcitation the system is basically nonequilibrium. Instead, a quasi-equilibrium 2D-electron accumulation layer is created, screening the semiconductor bulk from practically the entire electric field of the gate. The depletion layer accordingly disappears and neutral, hole-containing acceptors are found immediately beyond the accumulation layer. Since the wavefunction of 2D-electrons has a finite extent in the normal direction $z \| [001]$ to the interface ($\Psi(z) \sim z \exp(-bz/2)$, where $b^{-1} \approx 10$ Å), there is a finite probability of these electrons recombining radiatively with injected holes. But this recombination is indirect both in k-space and in real space. Hence its intensity should be extremely weak compared to the other radiative channels in the bulk. Experiments measure precisely this low intensity luminscence line, $2D_c$, which is 2-3 orders of magnitude weaker than corresponding lines from the bulk. In Fig. 8 we show luminescence spectra obtained in conditions of constant Ar laser illumination at $W_0 \approx 10^{-3}$ W/cm^2 power and varying gate voltages which change the 2D-electron concentration n_S. The concentration was simultaneously and independently measured by Shubnikov–de Haas oscillations. Omitting the details of the recombination mechanism, described in Ref. 67, we turn to the main properties of the $2D_c$ line without a magnetic field (see Fig. 8). First, this line appears in the spectrum only under laser illumination and gate voltages $V_g > V_T$ (V_T is the threshold voltage for the creation of a 2D-channel). The shape of the $2D_c$ line consists of an energy step function, reflecting the fact that the 2D-electron DS does not depend on E in the absence of a magnetic field. The width of the $2D_c$ line increases linearly with electron concentration n_S, while its ultraviolet cutoff is practically independent of the gate voltage. When 2D-electrons recombine with photoexcited holes assisted by TO- and TA-phonons the recombination probability does not depend on the energy of the recombining particles (matrix elements $M_{TO}, T_{TA} \approx$ const). Phonon replicas of the $2D_c$ line appear in the appropriate spectral regions. TO- and TA-phonon components of the $2D_c$ line are polarized in the 2D-plane, since only two of the six (001) electron valleys are populated with 2D-electrons. A very weak $2D_c$ line can also be observed in the phonon-free region of the spectrum because of recombination involving a transfer of momentum close to the Brillouin value, to an impurity center or the surface.

In the case of strong localization of 2D-electrons on random potential fluctuations (low concentration region)

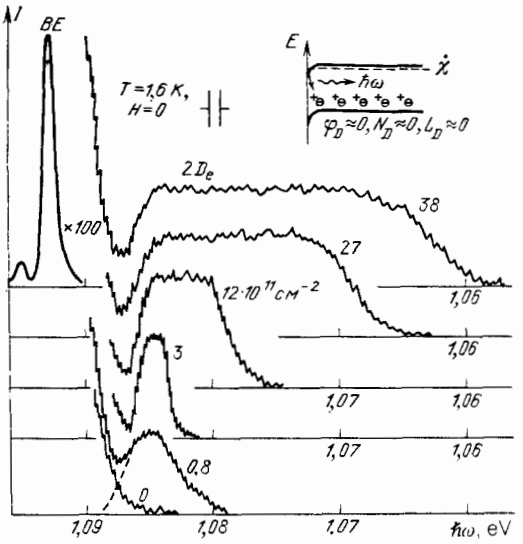

FIG. 8. TO-phonon components of the radiative spectrum measured in a Si(100)-MIS-structure at $T = 1.6$ K, $W = 10^{-3}$ W/cm^2 power density, and different positive bias potentials sufficient to form a 2D-electron channel.[67] 2D-electron concentration is measured simultaneously by magnetoconductance oscillations and is shown for each spectrum in units of 10^{11} cm^{-2}. The BE line is radiation from boron-bound excitons, the $2D_c$ line refers to radiative recombination involving 2D-electrons. The inset contains a schematic band diagram under photoexcitation (no depletion region) and shows a 2D-electron recombining with a hole on a neutral acceptor.

the $2D_c$ line becomes strongly broadened and unpolarized. Its width then reflects the amplitude of random potential fluctuations. Recombination rate of 2D-electrons with photoexcited holes is very low ($\sim 10^3$ s^{-1}). On this time scale the 2D-electron and hole subsystems are in thermal equilibrium with the lattice. The $2D_c$ line radiation spectrum consists of a convolution of 2D-electron and photoexcited hole distribution functions:

$$I(\hbar\omega) \sim \int_0^\infty F_e(E)\, F_h(\hbar\omega - E)\, dE,$$
$$F_{e(h)} = f_{e(h)} D_{e(h)}, \qquad (4.1)$$

where $f_{e(h)}$, $D_{e(h)}$ are the electron (hole) distribution function and density of states. Since the width of the experimentally measured[68] hole distribution function turns out to be small, not exceeding 0.8 meV, the $2D_c$ line spectrum accurately reflects the energy distribution of the single-particle 2D-electron density of states.

Now consider the main properties of the $2D_c$ line in a transverse magnetic field. In this case the $2D_c$ line is split according to the number of occupied Landau levels (Fig. 9). For example, spectrum 3 in Fig. 9 corresponds to the complete filling of four Landau levels at the given value of the magnetic field. Accordingly, the $2D_c$ line is split into four equidistant lines separated by the cyclotron energy $\hbar\omega_c = 4$ meV. The two-dimensionality of the electron system is verified by the standard procedure of tilting the magnetic field from the normal to the 2D-layer. Given constant n_S and H a tilt angle $\varphi = 60°$ exactly doubles the filling factor and the number of Landau levels under the Fermi surface doubles accordingly (see lower part of Fig. 9). By fitting the familiar Landau level fan diagram construction to the radiation spec-

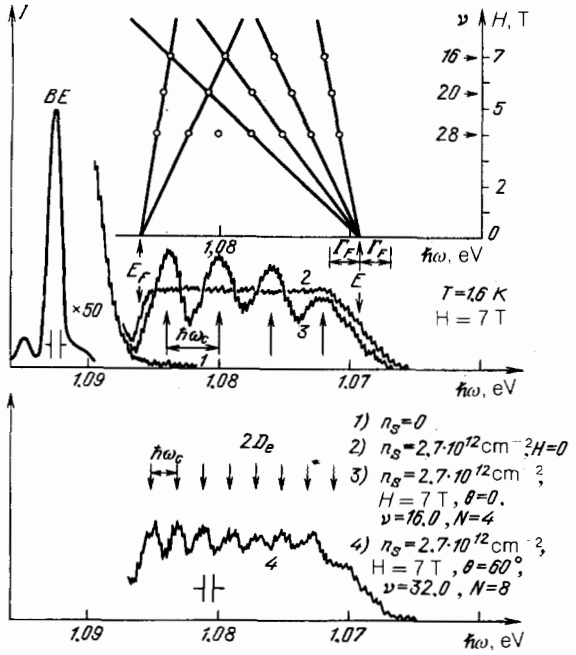

FIG. 9. Radiative recombination spectra of 2D-electrons with photoexcited holes ($2D_e$ lines).[67] Obtained from sample No. I at $W = 10^{-3}$ W/cm^2, $T = 1.6$ K, $n_S = 2.7\cdot10^{12}$ cm^{-2} and $H = 0$ (spectrum 2); $H = 7$ T perpendicular to the 2D-layer (spectrum 3); $H = 7$ T tilted from the normal by 60° (spectrum 4). Spectrum 1 was recorded with $n_S = 0$ ($V_g < V_t$). The BE line is radiation from boron-bound excitons; $\hbar\omega_c$ is the cyclotron splitting. The upper inset shows the Landau fan diagram (positions of spectral lines) constructed for $n_S = 2.10^{17}$ cm^{-2} with four, five and seven completely filled levels. Extrapolations H→O determine the bottom of the size-quantized band E_0 and the Fermi energy E_F.

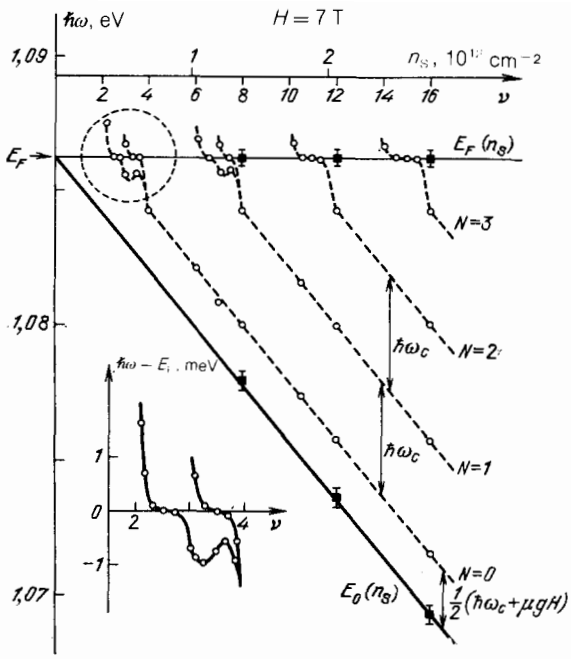

FIG. 10. Spectral position of the 2D-electron radiation lines as a function of concentration n_S. Measurements done on sample No. 3 at $W = 10^{-3}$ W/cm^2, $T = 1.6$ K, $H = 7$ T. Dark squares mark the positions of the Fermi energy E_F and the bottom of the band E_0 for different n_S, evaluated by the fan diagram technique at integral filling. The $2 < \nu < 4$ region is expanded in the inset. The observed line splitting is due to the nonequivalence of electron valleys.

trum recorded at different magnetic fields with $n_S = \text{const}$ and an integral filling factor, it is a simple matter to determine the positions of the bottom of the size-quantized band E_0 and the Fermi energy E_F. One such fan diagram is shown in the upper part of Fig. 9. The TO-phonon component of the $2D_e$ line in a transverse magnetic field is almost entirely polarized in the direction of H. Finally, at temperatures such that the paramagnetic hole splitting $g_h\mu_B H \ll kT$ only the lowest state with angular momentum projection $J_z = -3/2$ is populated. Then only 2D-electrons with spin projection $S_z = +1/2$ contribute to the recombination spectrum, because optical transitions involving $S_z = -1/2$ electrons are forbidden. This means that radiation spectra contain radiation corresponding to filling factors ν that satisfy $(2+4k) < \nu < (4+4k)$.

The shifts of spectral recombination line positions when concentration n_S (or filling factor ν) is varied at fixed H are shown in Fig. 10. Also shown are the measured dependence (dark squares) of the band bottom E_0 and Fermi energy E_F as a function of n_S. First, it is clear that at transverse $H = 7$ T we observe a series of Landau levels separated by $\hbar\omega_S$. The spectral position of the lines corresponding to Landau levels deep under the Fermi surface depends linearly on n_S and reflects the shift in the bottom of the band $E_0(n_S)$. Near the Fermi surface the odd integral ν give rise to two radiation lines, corresponding to 2D-electron recombination from different valleys (shown in detail in the inset to Fig. 10, see also Sec. 4.2). It is interesting to consider how the spectral position of the recombination lines is influenced by the quantization of Hall resistance,[2] arising from the pinning of the Fermi level at integral ν in a region of localized states in the gap between Landau levels. Figure 10 shows that the pinning of the spectral positions of the $2D_e$ lines is experimentally observed at half-integral ν. Yet no such effect is seen at integral filling. This behavior is easily explained by noting that at integral ν the DS at the Fermi level is small and E_F changes strongly with n_S, whereas at half-integral ν the quantity $D(E_F)$ is large and E_F does not change much.

The aforesaid properties of radiation recombination of 2D-electrons with photoexcited holes indicate that the optical spectroscopic method opens up new possibilities in the study of the 2D-electron energy spectrum and its variation with magnetic field, filling factor ν, temperature, and quality of structure. In the next section we will discuss how this method is employed to determine the magnitude of spin and intervalley splitting and to study the oscillatory behavior of these quantities as a function of the filling factor.

4.2. Oscillations of spin and intervalley splittings in the 2D-electron energy spectrum

The (2D-) electron system on the (100) surface of silicon is four-fold degenerate because of spin and the existence of two equivalent energy valleys.[1] However, the earliest experiments proved that this degeneracy is lifted by a transverse magnetic field and that the 2D-electron energy spectrum becomes completely discrete. This is manifested, for example, in the Shubnikov–de Haas oscillations wherein each of the four Landau sublevels (i.e., $\nu = 1, 2, 3, 4$ filling factors) gives rise to a minimum in magnetoconductance

because the Fermi level falls in the region of localized states between quantum sublevels. Different experimental methods were employed to determine the magnitude of spin and intervalley splittings. Some of these methods focused on the behavior of magnetoconductance in tilted H fields, thermally activated magnetoconductance (see Ref. 1), and contact potential difference.[41] Still, all these methods evaluated the splitting magnitude indirectly, making use of fitting parameters and assumptions requiring separate justification.

The optical spectroscopy method permits us to measure directly the magnitude of spin and intervalley splitting as the energy separation of the appropriate lines in the radiative recombination spectrum.

4.2.1. Intervalley splitting ΔE_v

A number of authors[70-72] calculated the intervalley splitting by ignoring electron-electron (e-e) interaction effects: the resulting quantity ΔE_v^0 was determined by the gate field. In these theories the intervalley splitting was a purely electrostatic phenomenon, arising from the nonequivalence of the two electron valleys with respect to the electric field vector. On the other hand, other studies[73-74] noted that the intervalley splitting should increase markedly in a transverse field H because of a term ΔE_v^* arising from 2D-electron interaction. Consequently, the full intervalley splitting ΔE_v contains two terms—Δ_v^0 and ΔE_v^*—and the contributions of ΔE_v^0 and ΔE_v^* depend differently on H, ν, and N.[1]

In the recombination spectrum of 2D-electrons at $\nu = 3.0$ and $T = 1.5$ K ($H = 7$ T) there exists a single line produced by the recombination of $S_z = +1/2$ 2D-electrons from the lower electron valley of the lowest Landau level ($N = 0$) (we have already seen that only ground state holes with $S_z = -3/2$ participate in recombination at low temperatures and that optical transitions involving $S_z = -1/2$ electrons are forbidden). If $\nu > 3$ electrons begin to occupy the next valley and a new line appears in the recombination spectrum (see Fig. 11). The intensity of this new line is proportional to the excess of ν over 3. The energy separation between the lines corresponds to the intervalley splitting ΔE_v. Thus the spectroscopic method not only makes it possible to measure ΔE_v directly, but also to measure the dependence $\Delta E_v(\nu)$.[75]

The dependence $\Delta E_v(\nu)$ measured at $H = 7$ T and $T = 1.6$ K is shown in Fig. 12. Clearly the quantity $\Delta E_v(\nu)$ oscillates strongly, peaking at odd integral $\nu = \nu^* = 3, 5, \ldots$. The absolute magnitude of $\Delta E_v(\nu)$ measured by optical spectroscopy markedly exceeds the values obtained by other methods (see Refs. 1, 41). Moreover, ΔE_v decreases as ν shifts from ν^*, indicating the filling of a new valley. This behavior argues for an intervalley splitting mechanism based on e-e interaction and contradicts the notion of nonrenormalized ΔE_v. Indeed, according to Ref. 73, ΔE_v is enhanced because 2D-electrons from different valleys have different quantum numbers and are not forbidden by the Pauli exclusion principle from sharing the same spatial region. This leads to additional Coulomb repulsion and enhances ΔE_v by ΔE_v^*. If the valley Landau sublevels are equally filled (i.e. at even integral $\nu = \nu^0 = 2, 4, 6 \ldots$) ΔE_v^* turns to zero[73] and ΔE_v is minimized. Consequently the dashed line in Fig. 12 corresponds to the dependence of nonrenormalized ΔE_v^0 on n_s. The experimentally measured function $\Delta E_v^0(n_s)$ turned out to be universal and independent of H. The ΔE_v^* term, on the other hand, depends strongly on H and quantum level N, as is evident in Fig. 12.

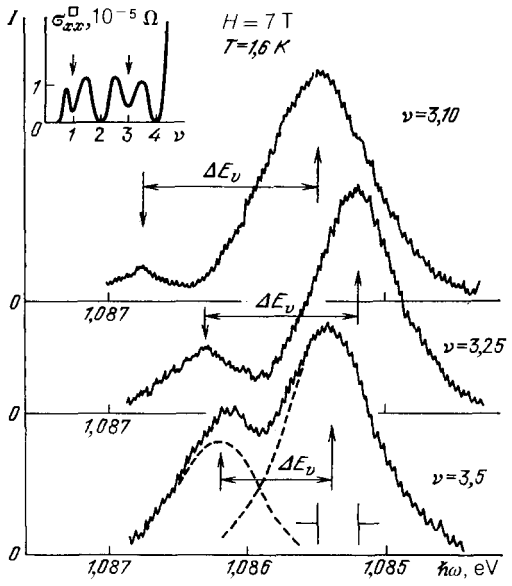

FIG. 11. Radiative recombination spectra of 2D-electrons, obtained from sample No. 2 at $H = 7$ T, $T = 1.6$ K, $W = 10^{-3}$ W/cm^2, and different $\nu = 3.1$, 3.25, and 3.5. ΔE_v indicates the magnitude of intervalley splitting. The inset shows the $\sigma_{xx}(\nu)$ dependence measured simultaneously at the same H, T, and W parameters.

4.2.2. Spin splitting ΔE_s

As we have seen, at low temperatures in strong magnetic fields the recombination spectrum of 2D-electrons contains only a single spin component with the $S_z = +1/2$ spin projection, while electrons with $S_z = -1/2$ do not radiate. This happens because the Zeeman effect splits the hole level into a quartet and at low temperatures all nonequilibrium holes have time to collect in the ground state with $J_z = -3/2$. Optical transitions involving $S_z = +1/2$ electrons and $J_z - 3/2$ holes are forbidden by the selection rules and the corresponding radiation line is not observed. In order to observe the recombination of $S_z = +1/2$ 2D-electrons (and consequently determine the spin splitting $\Delta E_s \equiv g_e \mu_B H$) the temperature must be raised, leading to an appreciable population of $J_z = -1/2$ holes.

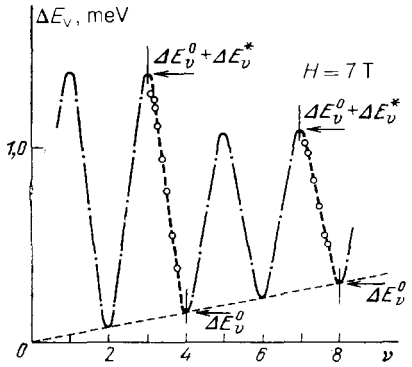

FIG. 12. Intervalley splitting ΔE_v as a function of filling factor ν, measured at $H = 7$ T, $T = 1.6$ K.

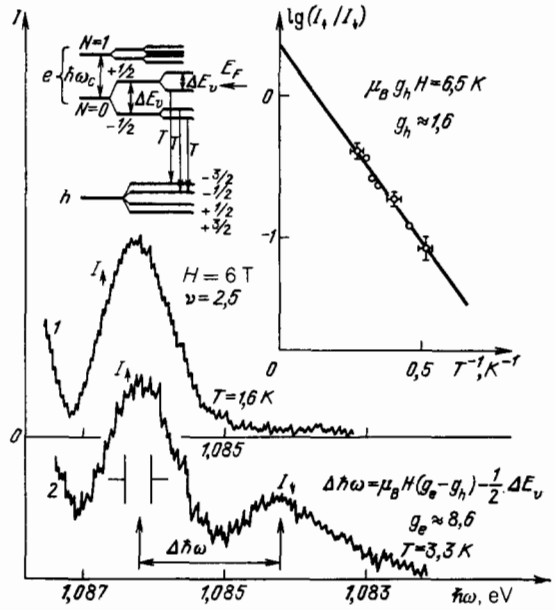

FIG. 13. Radiative recombination spectra of 2D-electrons, obtained from sample No. 2 at $H = 6$ T, $\nu = 2.5$, $W = 10^{-3}$ W/cm^2 and $T = 1.6$ K (spectrum 1) or $T = 3.3$ K (spectrum 2). The value $\Delta\hbar\omega$ is determined by the spin splitting ΔE_S. The level diagram shows electron and hole splittings in the magnetic field and the allowed optical transitions. The inset shows the temperature dependence of the $I\uparrow/I\downarrow$ intensity ratio.

At $H = 6$ T, $\nu = 2.5$, and $T = 1.6$ K the radiation spectrum contains but a single line produced when 2D-electrons from the lower valley with $S_z = +1/2$ recombine with $J_z = -3/2$ holes. When the temperature is raised to 3.3 K a second radiation line appears in the low-energy section of the spectrum (see Fig. 13). This line is produced by $S_z = -1/2$ electrons recombining with $J_z = -1/2$ holes.[68] The intensity of this line falls exponentially with temperature (see inset of Fig. 13), which makes it possible to evaluate the g-factor of the recombining holes. The energy separation between the lines in Fig. 13 (spectrum 2) reflects the 2D-electron spin splitting. At $H = 6$ T, $\nu = 2.8$, and $T = 3.3$ K, the 2D-electron g-factor evaluated by this method turned out to be $g_e = 8.6$, significantly larger than the bulk value $g_e^0 = 2$. Just as in the case of intervalley splitting, this enhancement of g_e for 2D-electrons is undoubtedly due to e-e interaction effects.[29] This conclusion is supported by the $g_e(\nu)$ dependence, plotted in Fig. 14 for $H = 7$ T. Clearly the 2D-electron g-factor oscillates strongly with ν, reaching maximum values at $\nu = 2$, 6, 10 . . . and minimum ($g_e^0 = 2$) values at equal filling of spin component states (i.e. at $\nu = 4$, 8, 12 . . .).

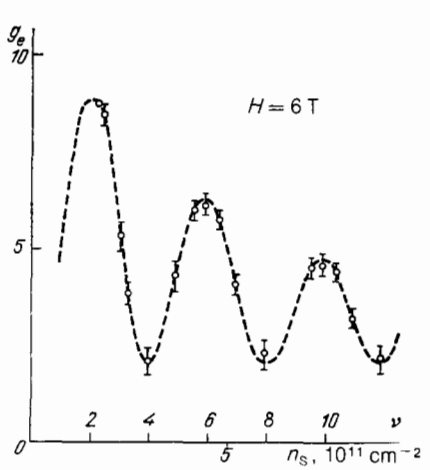

FIG. 14. 2D-electron g-factor as a function of filling factor ν and concentration n_S, measured at $H = 6$ T and $T = 1.6$–3.3 K.

In this manner, the optical spectroscopy method provides a means of directly measuring the magnitude of spin and intervalley splittings, which were found to oscillate strongly as a function of filling factor ν.

4.3. Oscillations in the 2D-electron density of states in a transverse magnetic field

The screening of the random potential produced by defects is most clearly manifested in the oscillations of the radiative recombination line broadening on Landau levels as a function of the filling factor, as well as in the temperature behavior of the recombination spectra. These effects merit separate discussions.

4.3.1. Oscillations of Landau level broadening as a function of filling factor

The spectra corresponding to the filling factors $\nu = 2.5$, 3.5, and 4.0 in the lowest Landau level are shown in Fig. 15. The doublet nature of the $\nu = 2.8$ spectrum is due to the valley-orbit splitting ΔE_v. At $\nu = 2.8$ the lower energy state, corresponding to $S_z = +1/2$, is entirely filled, whereas the higher energy state with the same spin projection is higher in energy by ΔE_V and is only half-filled. Consequently the intensity of the shorter wavelength doublet component, corresponding to the higher energy-split state, is twice as weak as its long-wavelength counterpart (in Fig. 15 the contours of these doublet components are separated by dashed lines).

By comparing the recombination spectra of Fig. 15 it is easy to see that the linewidth does not depend monotonically on the filling of Fig. 15 it is easy to see that the linewidth does not depend monotonically on the filling of the electron

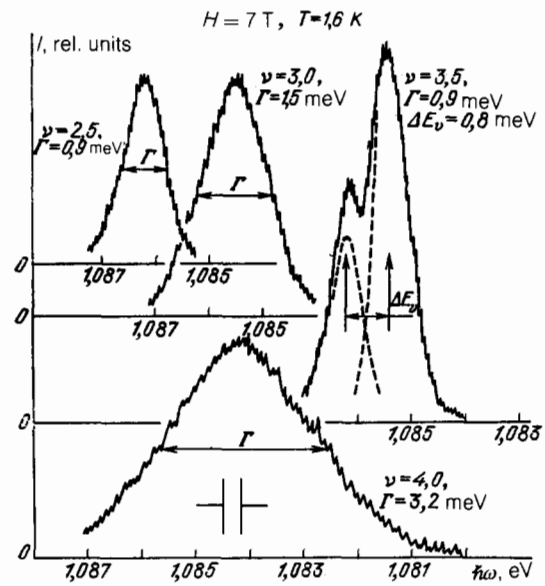

FIG. 15. Radiative recombination spectra of 2D-electrons, recorded on sample No. 1 at $H = 7$ T, $T = 1.6$ K, and $W = 10^{-3}$ W/cm^2 for various filling factors of the lowest Landau level ($N = 0$).

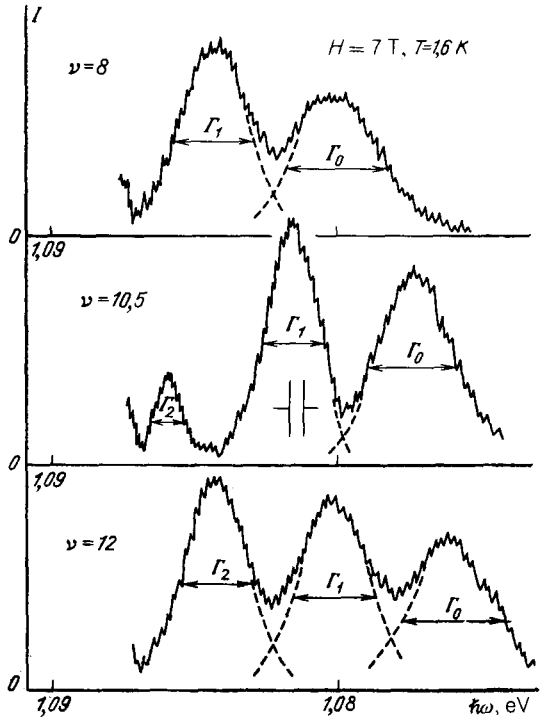

FIG. 16. Radiative recombination spectra of 2D-electrons, obtained from sample No. 1 at $H = 7$ T, $T = 1.6$ K, and $W = 10^{-3}$ W/cm^2 for different fillings of the $N = 2$ Landau level.

states: at full occupation (integral ν) the lines are much broader than at half occupation. A qualitatively analogous dependence on ν is exhibited by recombination spectra of systems in which several Landau levels are completely full and the population of the most energetic level is varied. In Fig. 16 we show recorded spectra with the lowest two Landau levels ($N = 0, 1$) completely filled and the occupation of the upper $N = 3$ level varies. Once again, the linewidth of all spectral lines does not depend monotonically on ν—at integral ν the lines are much broader than at half-integral ν. Also, it is evident that when several Landau levels are completely filled the linewidth increases monotonically as the quantum number N decreases.

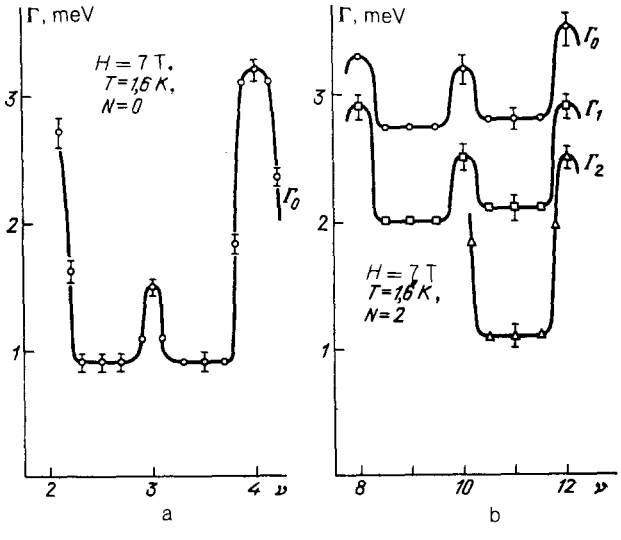

FIG. 17. Landau level broadening Γ vs filling factor ν, measured on sample No. 1 at $H = 7$ T, $T = 1.6$ K for the $N = 0$ (a) and $N = 2$ (b) Landau levels.

The oscillating behavior of the recombination linewidth as a function of ν when one or several Landau levels are involved is illustrated in Fig. 17, a,b. These oscillations have the greatest amplitude when only one (the lowest) Landau level is involved. When several Landau levels are filled similar oscillations are observed, but the lower the level under the Fermi surface (lower N), the smaller their magnitude. The observed recombination linewidth oscillations are a direct consequence of oscillating broadening of the peaks in the density of states on Landau levels as a function of electron concentration. The mechanism behind this phenomenon undoubtedly involves random potential screening.

Let us discuss this question in more detail. At integral ν the Fermi level falls precisely at the midpoint of a gap in the energy spectrum. Then electrons fill the Landau levels completely and the screening is diminished. In the absence of screening the Landau levels "trace" the potential profile determined by long-period fluctuations. If we assume that these fluctuations are caused by charged defects in the SiO_2 dielectric layer, then nonequilibrium holes that recombine with 2D-electrons are less affected by these fluctations because they are quite distant from the Si-SiO_2 interface ($\geqslant 10^2$ Å). The logical conclusion is that at integral filling the radiative linewidth is determined by the charge fluctuations in the dielectric, since the electrons that participate in recombination are distributed in energy within the given Landau level according to the potential profile.[68] Significantly, the measured linewidths in the case of full occupation of the lowest Landau level in several MIS-structures are practically identical to the linewidths ΔE measured in the strong localization regime at $H = 0$. These latter linewidths also probe the amplitude of large-scale fluctuations.[67]

It is useful to note that in cyclotron resonance (CR) measurements, unlike the luminescence technique discussed here, large-scale fluctuations of the random potential with $d > l_H$ do not contribute to the CR linewidth.

At half-integral filling the Fermi level coincides with a peak in the density of states (the maximum of the radiative spectral line). In this area of the energy spectrum the states are extended. Now electrons screen large-scale random potential fluctuations most effectively and consequently the potential profile produced by these fluctuations is smoothed out. The linewidth of the luminescence peak should shrink accordingly, in full agreement with experiment (see Fig. 15). The finite width of the DS peak in these circumstances is determined by the small-scale random scatterers which remain unscreened. The experimentally recorded luminescence peak linewidths $\Gamma \approx 0.8$ meV at half-integral ν (see Fig. 17) were much larger than could be expected from the small-scale scatterers at the given H and μ.[1,23] In fact, the minimum linewidth Γ measured in these experiments is determined by the energy distribution of nonequilibrium holes which recombine with electrons. Once the hole-induced broadening is taken into account,[68] it turns out that the true width of the luminescence peaks, which reflect the width of DS peaks at Landau levels, should be much narrower at half-integral ν. This indicates that the actual magnitude of oscillations in the DS peak width as ν is varied should be approximately three times larger than experimentally observed (see Fig. 17).

Oscillations in Γ with filling factor were predicted in Refs. 26, 27, 34. The nature of these oscillations was associated with the periodically varying screening radius. No analytic expressions for Γ were derived in these papers.

Recently Shklovskiĭ and Efros developed a theory of nonlinear screening of charged center potentials by electrons, with the charged centers randomly distributed in the bulk with concentration n_3.[38] The centers are taken to produce Coulomb potentials and screening is described by charge fluctuations on the scale L. At integral Landau level filling there is no screening. Screening appears when the 2D-electron concentration n_S deviates from the concentration n_S^0 which corresponds to integral filling $\delta n_S = n_S - n_S^0$). If the number of excess electrons in the plane $\delta n_S L^2$ for a given scale L equals the fluctuation in the number of the charged centers in the bulk $(n_3 L^3)^{1/2}$, then on all scales larger than L the random potential is completely screened by electrons. The screening length changes with the number of electrons δn_S, so in a sense the scale L represents the nonlinear screening radius. The dependence of the Fermi level and the width of the DS peak at the Landau level on the electron concentration in a magnetic field is derived in Ref. 35. An important result of this nonlinear screening theory is that the density of states in the gaps between Landau level is not exponentially small, as it should be in the case of a short-range random potential[1,23] or in the case when the charged centers are located in a 2D-plane.[33] This happens because the charged centers in the bulk are more important than surface centers: as δn_S decreases the random potential comes to involve other bulk centers in a layer of thickness L, which grows rapidly.

The theory of Ref. 35 qualitatively explains the main experimental results related to the oscillations in the density of states as a function of electron concentration, which were discovered from the luminescence spectra. In particular, it follows[35] that when the amplitude of the large-scale fluctuations reaches the magnitude of the appropriate gap in the energy spectrum ($\hbar\omega_c$, ΔE_S or ΔE_V) the two adjacent Landau sublevels begin to participate in the screening and the width of the DS peak ceases to grow, since it is limited by the magnitude of the energy gap. It has been observed experimentally (see Fig. 17) that the luminescence linewidth at integral filling ($\nu = 4$) is much larger than in the case of $\nu = 3$, because the energy gap at $\nu = 4$ ($\hbar\omega_c \approx 4$ meV) is markedly larger than at $\nu = 3$ ($\Delta E_V \approx 1.5$ meV)[75]. The formulae of Ref. 35 can be combined with the parameters of the studied MIS-structures to estimate the amplitude and range of the random potential fluctuations (see Sec. 4.4).

4.3.2. Temperature dependence of Landau level broadening

As we have noted earlier, if N Landau levels of a 2D-electron system in a transverse magnetic field are completely filled then the electrons are uniformly distributed over the area of the system and no screening occurs. Screening appears if some number of excess electrons (or holes) is introduced into the system. The creation of these electrons and holes need not involve changes in n_S or H, for raising the temperature at constant n_S and H has the same effect. Therefore, the experimentally observed radiative linewidths corresponding to integral Landau level filling (i.e., when $n_S = veH/h$, ν an integer) should become narrower as the temperature is raised. Since the concentrations of thermally activated electrons and holes are equal

$$\delta n_e = \delta n_h \sim \exp\left(-\frac{\hbar\omega_c}{2kT}\right), \tag{4.2}$$

this effect can only be observed if $\hbar\omega_c$ and kT are comparable.

The radiative spectra recorded at $n_S = 4\cdot10^{11}$ cm^{-2}, $\mu = 2.6\cdot10^4$ cm^2/V·s, in fields $H = 0$ (spectrum 1) and $H = 2.5$ T (spectrum 2) at $T = 1.5$ K are shown in Fig. 18. First of all, it is immediately apparent that even though the parameter μH is much larger than 1 (in this experiment $\mu H = 6.5$) the Landau level structure does not apear in the spectrum. This is so because the level broadening (which can be obtained from the high-energy tail of the $2D_e$ line) practically equals the cyclotron splitting. This property is common to all studied structures: at low magnetic fields the luminescence linewidth is close to $\hbar\omega_c$, then as H increases $\hbar\omega_c$ approaches the amplitude Q of random potential fluctuations and the linewidth Γ saturates, leading to well-resolved Landau levels. This dependence $\Gamma(H)$ agrees with the theory of nonlinear screening of long-range random potential fluctuations.[38]

Spectrum 3 of Fig. 18 was taken at a higher temperature $T = 3.8$ K. The high-temperature narrowing of Landau levels as electrons and holes appear in the sublevels is evident in this spectrum. The temperature-induced filling of the uppermost level is accompanied by the appearance of an additional radiative line shifted towards higher energies by $\hbar\omega_c$ (see Fig. 18, spectrum 3).

Thus we find that the variation of Landau level broadening with temperature and filling factor is explained by the screening of defect-induced long-range random potential fluctuations, in qualitative agreement with the theory of Ref. 35.

4.3.3. Width of the luminescence peak at half-integral Landau level filling

At half-integral filling of quantum states the long-range potential fluctuations are screened and the width of the DS

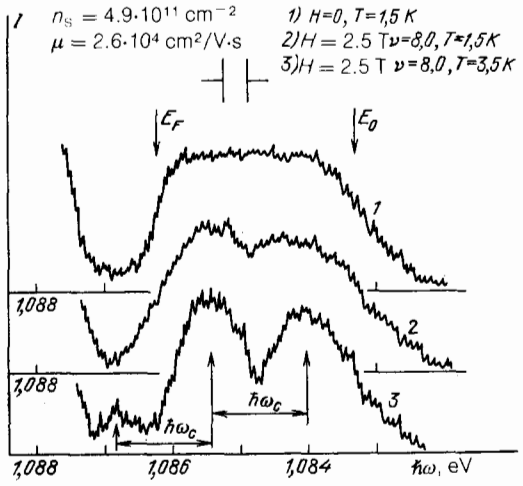

FIG. 18. Radiative recombination spectra of 2D-electrons, obtained from sample No. 1 at $n_S = 4.9\cdot10^{11}$ cm^{-2}, $\mu = 2.6\cdot10^4$ cm^2/V·s, $W = 10^{-3}$ W/cm^2 and various values of H and T: $H = 0$, $T = 1.5$ K (spectrum 1); $H = 2.5$ T ($\nu = 8$), $T = 1.5$ K (spectrum 2); and $H = 2.5$ T, $T = 3.3$ K (spectrum 3).

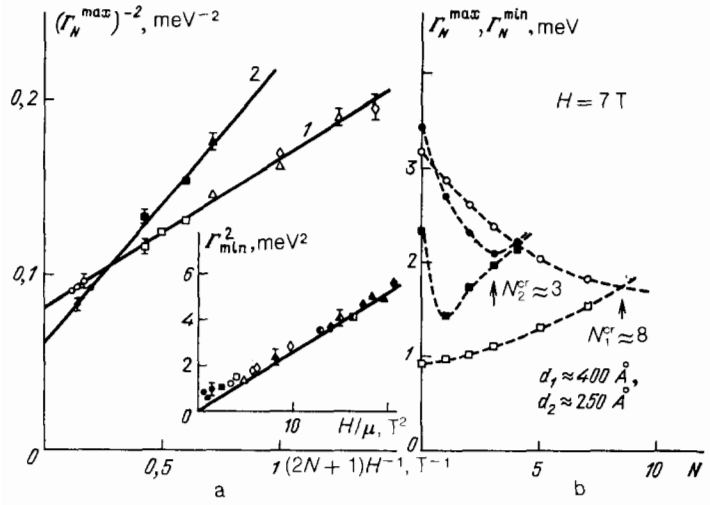

FIG. 19. a—Width Γ_N^{max} of the Nth Landau level at integral filling of N levels in different magnetic fields for two samples (light and dark symbols) as a function of the parameter $(2N+1)H^{-1}$. Different symbols label different quantum numbers N: $N=0$ (circles), $N=1$ (squares), $N=2$ (triangles), $N=3$ (diamonds). b—Γ_N^{max} (circles) and Γ_N^{min} (squares) as functions of the Landau level number N, measured at $H=7$ T and $T=1.6$ K on the same structures; the inset shows Γ_{min}^2 as a function of the parameter H/μ for four different structures (different symbols) and different quantum numbers N (light and dark symbols).

peaks are narrowed towards their minimum value Γ_{min}. If interaction with short-range scatterers becomes dominant then, according to the theory,[1,23] the quantity Γ_{min} should depend on the single parameter H/μ. Consequently it is of interest to follow the variation in the broadening of the DS peak, which can be obtained from an analysis of the luminescence line, with variation in the parameter H/μ.

The dependence of the DS peak width on H/μ at half-integral filling is shown in the inset of Fig. 19 depicting Γ_{min}^2 as a function of (H/μ). The experimental points plotted in that graph were obtained from measurements on different structures with different quantum numbers N (hence the different symbols). Nonetheless they are all well described by a universal dependence that can be approximated by a straight line. This behavior indicates that at half-integral ν the width of the DS peak is related to scattering from small-scale fluctuations. Moreover, it follows from the data that the peak width is independent of the quantum state number. Absolute values of Γ_{min} measured experimentally at given H and μ approach the theoretical values calculated in Refs. 1, 23.

In the region of small H/μ values (inset of Fig.19) the experimental dependence $\Gamma_{min}^2(H/\mu)$ deviates appreciably from the straight line and the symmetric lumiscence line tends towards a finite linewidth as $(H/\mu)\to 0$. This finite quantity is directly related tothe energy width of the non-equilibrium hole distribution (≈ 0.8 meV).[68]

4.4. Determination of the amplitude and spatial extent of the random defect potential

As we have noted in Sec. 4.3, if the level broadening is much smaller than the energy gap ($\Gamma \ll \hbar\omega_c$) at integral filling then the density of states on a single level reflects the energy distribution of long-range random potential fluctuations. Consequently, the fluctuation amplitude Q can be extracted from the recombination linewidths in the luminescence spectrum. It should be noted, however, that electrons will localize on random potential fluctuations if the fluctuation scale d exceeds the electron cyclotron radius $l_H(2N+1)^{1/2}$, where l_H is the mangetic length.[1] Therefore the Landau level broadening should reflect the fluctuation amplitude only if the $d \gg l_H(2N+1)^{1/2}$ and $\hbar\omega_c \gg q$ conditions are satisfied. In the more general case, when $d \geqslant l_H(2N+1)^{1/2}$, the broadening Γ is smaller than Q and depends on the $d^2/l_H^2(2N+1)$ ratio according to the expression

$$\Gamma = Q\left[1 + \frac{l_H^2(4N+2)}{d^2}\right]^{-1/2}. \qquad (4.3)$$

Expression (4.3) was derived for the ground state Landau level in Ref. 15 and for the higher lying levels N in Ref. 17. This formula can be applied to determine the parameters d and Q for the luminescence spectra of various structures. It should be recalled, however, that formula (4.3) ignores screening effects and consequently is only valid given the following: first, integral filling and, second, $\hbar\omega_c > Q$, i.e., when the Landau level structure is well-resolved in the luminescence spectrum. In Fig. 19a we illustrate the dependence $\Gamma^{-2}(H,N)$ for two structures plotted as Γ^{-2} as a function of $(2N+1)H^{-1}$. In these curves the points obtained for different values of N are well described by a straight line. The slope in these coordinates determines d and the y-intercept determines Q. Characteristically, two structures of different quality are characterized by different parameters d and Q: the lower quality structure (judging by the maximum mobility) exhibits higher fluctuation amplitude Q and smaller spatial scale d. The scale of long period fluctuations of the random defect potential can be evaluated independently of other measurements. If the field H is held constant and the ratio of Landau level broadening at integral filling (Γ_{max}) and half-integral filling (Γ_{max}) is measured with increasing N, then the quantities Γ_{max} and Γ_{min} can be expected to approach one another. Indeed, the cyclotron radius increases with N and for cyclotron orbits with $l_H(2N+1)^{1/2} > d$ potential fluctuations of linear extent d will become small-scale. As a result the difference between Γ_{max} and Γ_{min} should disappear.

The changes in Γ_{max} and Γ_{min} with N (for the same two structures as in Fig. 19a) in a field $H=7$ T is shown in Fig. 19b. The increasing tendency in $\Gamma_{min}(N)$ is due to a decrease in 2D-electron mobility at larger n_s. Clearly, as N increases the values of Γ_{max} and Γ_{min} approach one another and become equal at some $N = N_{cr}$. A likely interpretation is that at this quantum number the fluctuation scale d becomes comparable to the electron cyclotron radius $l_H(2N_{cr}+1)^{1/2}$, which yields a quick estimate of d. If the

various estimates of d are compared we find that different methods of evaluating the scale of long-range potential fluctuations yield consistent results for all studied structures.[68] Moreover, the fluctuation amplitudes of ΔE measured at $H = 0$ and the values of Q extracted from the $\Gamma(H)$ dependence are in good agreement.[68]

One of the most important questions that enter into evaluating the parameters d and Q arises from the fact that the long-period part of the conduction band profile near the interface could be partially repeated in the bulk, i.e. in the region containing nonequilibrium holes. In fact, the 2D-electron system effectively screens the external electric field produced by the full charge of the system, but not the sign-varying part of the long-period charge fluctuations. It was shown in Ref. 68 that hole level broadening due to potential fluctuationms on the $d < 500$ Å scale is insignificant and cannot alter the interpretation or significantly shift the parameters of the spectroscopic method. The same conclusion is reached by the following qualitative argument. Suppose potential fluctuations are significant in the valence band containing nonequilibrium holes. This implies that the optically measured luminescence linewidth should be markedly narrower than the actual Landau level broadening Γ. At the same time, our understanding of nonlinear screening requires that Γ not exceed $\hbar\omega_c$ and therefore all optically measured linewidths at integral filling are always much smaller than $\hbar\omega_c$. But this contradicts experimental results (see Fig. 18). We conclude, therefore, that the real values of d in studied structures are not too large, so that random potential fluctuations do not have a great effect on the valence band where the holes are located. On the other hand, it is equally clear that potential fluctuations on the $> 10^3$ Å scale are almost entirely reproduced by the valence band profile at a distance $z = 100$ Å from the interface. These fluctuation scales are therefore not probed by the discussed luminescence method.

Thus we have seen that the optical spectroscopic method not only distinguishes the effect of long-period random defect potential fluctuations on the Landau level broadening oscillations, but also permitted the first evalution of the amplitude and range of these fluctuations from the dependence of Landau DS peak broadening on the magnetic field and quantum number.

4.5. Evaluating the overall density of states

As we have noted earlier (Sec. 3), at integral Landau level filling (in the quantum Hall effect regime)[2] different methods can be used to determine the thermodynamic DS. All these methods lead to the same conclusion: the density of states in the energy gaps is not exponentially small, but rather makes up a significant part of the H = 0 density of states. This has been explained in the following manner:[6,52] the 2D-electron density of states consists of a superposition of narrow Gaussian peaks centered at the Landau levels on an energy-independent DS background. This formal explanantion appears unconvincing and essentially harks back to the "reservoir model"[76] originally proposed to explain the Hall effect and then rejected as inadequate for describing the QHE. We prefer the more natural explanation based on the oscillation of Landau level broadening as a function of ν. In this model the Landau levels are strongly broadened at integral filling by the long-range random potential fluctuations and consequently the DS remains large between the Landau levels. At half-integral filling, when the Fermi level falls in the region of extended states and long-range fluctuations are screened, the Landau levels are narrower and the DS becomes very large at the Fermi level and exponentially small between the Landau levels.

It is interesting to compare quantitatively the overall 2D-electron DS measured by completely different means, for example by mangetooptics and by the thermally activated magnetoconductance. It should be realized immediately that these methods measure different quantities. While the optical spectroscopy of 2D-electrons probes the entire $D(E)$ dependence and can be used to evaluate the quantity $D(E_F)$, the rest of the methods focus on the thermodynamic DS—i.e., on the quantity dn_s/dE_F, which is generally not equivalent to $D(E_F)$. Still, when E_F is located at a $D(E)$ minimum the quantities DE_F and dn_s/dE_F should be close,[31] so the two quantities can be compared at integral ν.

Now let us turn to the problem of quantitatively determining the DS using radiative recombination spectra.[67,68] The procedure is based on comparing the spectrum measured at integral filling of N Landau levels with the $H = 0$ spectrum recorded at the same concentration n_s. In order to evaluate the constant relating intensity and DS recall that at $H = 0$ the $2D_e$ line shape is a step-function in energy, reflecting the constant zero-field 2D-electron DS: $D = m/\pi\hbar 2 = D_0$. Hence the intensity scale can be calibrated in terms of DS values. The quantitative evaluation of $D(E)$ and $D(E_F)$ can subsequently be accomplished by comparing the radiative spectrum in a magnetic field with the zero-field spectrum at the same 2D-electron concentration n_s. As n_s is held constant, the integrated intensity of both spectra should be the same.

As an example of this method, in Fig. 20 we show how the density of states, its energy distribution and the value of $D(BE_F)$ (see Fig. 20,b) can be quantitatively established by comparing radiation spectra for $n_s = 1.36 \cdot 10^{12}$ cm^{-2}, $T = 1.6$ K at $H = 0$ (spectrum 1 in Fig. 20,a) and at $H = 7$ T (spectrum 2, $\nu = 6$). We note that in this example there are no additional difficulties arising from intervalley and spin splitting, since at low temperatures only one spin component of the electron distribution participates in recombination and the intervalley splitting is practically nonexistent: $\Delta E_v = 0.3$ meV.[75] The dashed lines in Fig. 20,b show the Landau level contours. A convolution of these with the $f_h(E)$ function (measured independently at $\mu H = 50$, when $\Gamma_{min} \to 0$) exactly matches spectrum 2 of Fig. 20,a. The dash-dotted line in Fig. 20,b shows the next, unfilled Landau level, whereas the solid line marks the overall density of states in the gaps between levels. We see that in these conditions ($H = 7$ T, $\nu = 8$, $\mu H = 11$) the quantity $D(E_F) = 0.32D_0$.

We also measured the thermodynamic DS of these structures by the activated magnetoconductance method (see Sec. 3.5). Since we wanted the value of thermodynamic DS precisely half-way between Landau levels (only near a minimum in $D(E)$ are the quantities $D(E_F)$ and dn_s/dE_F close), we had to consider both electronic and hole contributions to magnetoconductance (see Ref. 58). The temperature dependence of the magnetoconductance measured near the DS minimum is described by expression (3.13). Whereas the magnetooptical measurements described in Fig. 20 yield-

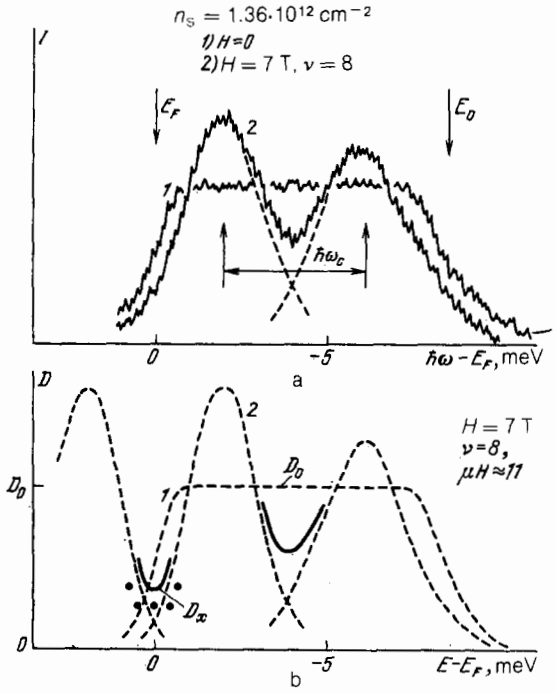

FIG. 20. a—Recombination spectra of 2D-electrons obtained from sample No. 2 at $H = 0$ (spectrum 1) and $H = 7$ T (spectrum 2), with $n_S = 1.36 \cdot 10^{12}$ cm^{-2}, $\mu = 1.6 \cdot 10^4$ cm^2/V·s, $W = 10^{-3}$ W/cm^2, $T = 1.6$ K. b—energy distribution of the density of states on the Landau levels (dashed lines) and total $D(E)$ (solid lines) extracted from the spectral lineshapes. The points indicate the values of dn_S/dE_F measured simultaneously by the thermally activated magnetoconductance technique at the same parameters.

ed a value $D(E_F) = 0.32D_0$, the DS obtained by the thermally activated magnetoconductance turned out to be somewhat smaller: $dn_S/dE_F = 0.28D_0$ (changes in dn_S/dEF with E_F are also shown in Fig. 20,b).

Thus we find that at integral Landau level filling the quantities $D(E_F)$ and dn_S/dE_F measured by completely different experimental techniques are in adequate agreement. The small discrepancy in the two values can be explained in several ways. More importantly, at integral ν the quantities $D(E_F)$ and dn_S/dE_F are analogously affected by changes in μ, H or structural parameters.[68]

The behavior of the density of states between the Landau levels as a function of magnetic field can be described as follows: in strong magnetic fields, when $\mu H > 1$ but the cyclotron splitting is smaller than the amplitude of long-range random potential fluctuations $\hbar\omega_c < Q$, the broadening Γ is of the order of $\hbar\omega_c$ and the DS in the gaps makes up a significant fraction of D_0. If these conditions are fulfilled the density of states in the gaps does not drop exponentially as magnetic field is increased, but falls off more slowly, perhaps by a power law.[35] When the magnetic field reaches such values that $\hbar\omega_c \geqslant Q$, the broadening Γ saturates and tends towards Q, while the DS in the gaps begins to fall exponentially with increasing magnetic field. As a consequence, optical methods are not the only means of measuring the amplitude of the random potential fluctuations—thermally activated magnetoconductance, for example, can also be employed in this regard.

5. CONCLUSION

In this review we have discussed the main theoretical concepts used to describe the density of states of a 2D-system in a magnetic field, as well as the experimental methods of measuring this density of states. This field of research, as well as the entire range of questions associated with the quantum Hall effect, is far from exhaustively studied and is constantly evolving. At the same time, the structure of the energy spectrum of real 2D-systems and the mechanisms responsible for this structure are to some extent understood. In conclusion it is proper to delineate the problems that appear most promising and fundamental for future study. In our opinion, these problems include: the behavior of the density of states in the regions of fractional filling and its connection with the fractional QHE; development of stronger magnetic field sources for more detailed studies of the random potential; a rigorous calculation of the linear screening coefficient; calculation and experimental verification of the Fermi-liquid effects; and a detailed study of the shape of the peaks in the single-particle density of states.

[1]T. Ando, A. B. Fowler, and F. Stern, Rev. Mod. Phys. **54**, 437 (1982).
[2]K. Klitzing, G. Dorda, and M. Pepper, Phys. Rev. Lett. **45**, 494 (1980).
[3]D. C. Tsui, H. L. Störmer, and A. C. Gossard, Phys. Rev. Lett. **48**, 1559 (1982).
[4]É. I. Rashba and V. B. Timofeev, Fiz. Tekh. Poluprovodn. **20**, 977 (1986) Sov. Phys. Semicond. **20**, 617 (1986)].
[5]J. P. Eisenstein, H. L. Störmer, V. Narayanamurti, A. Y. Cho, and A. C. Gossard, Phys. Rev. Lett. **55**, 678 (1985).
[6]E. Gornik, R. Lassnig, G. Strasser, H. L. Störmer, A. C. Gossard, and W. Wiegmann, Phys. Rev. Lett. **54**, 1820 (1985).
[7]E. Stahl, D. Weiss, G. Weimann, K. Klitzing, and K. Ploog, J. Phys. C **18**, L783 (1985).
[8]I. V. Kukushkin and V. B. Timofeev, Pis'ma Zh. Eksp. Teor. Fiz. **43**, 367 (1986) JETP Lett. **43**, 499 (1986)].
[9]A. A. Abrikosov, L. P. Gor'kov, and I. E. Dzyaloshinskiĭ, *Methods of Quantum Field Theory in Statistical Physics*, Prentice-Hall, Englewood Cliffs, NJ, 1963 [Russ. original, Fizmatgiz, M., 1962].
[10]I. B. Levinson, A. Yu. Matulis, and A. M. Shcherbakov, Zh. Eksp. Teor. Fiz. **60**, 859 (1971) [Sov. Phys. JETP **33**, 464 (1971)].
[11]V. L. Bonch-Bruevich and R. Rozman, Fiz. Tverd. Tela Leningrad **5**, 2890 (1963) [Sov. Phys. Solid State **5**, 2117 (1964)].
[12]J. E. Furneaux and T. L. Reinecke, Phys. Rev. B **33**, 6897 (1986). R. J. Hang, K. Klitzing, and K. Ploog, Phys. Rev. B **35**, 5933 (1987).
[13]T. Ando, J. Phys. Soc. Japan 36, 1821 (1974); **37**, 622, 1233 (1975).
[14]R. R. Gerhardts, Z. Phys. Kl. B **21**, 278 (1975); Surf. Sci. **58**, 227 (1976).
[15]S. Hikami and E. Brezin, J. Phys. (Paris) **46**, 2021 (1985); Surf. Sci. **170**, 262 (1986).
[16]K. A. Benedict and J. T. Chalker, J. Phys. C **19**, 3587 (1986).
[17]T. Ando, J. Phys. Soc. Japan **52**, 1740 (1983); **53**, 3101, 3126 (1984).
[18]F. Wegner, Z. Phys. Kl. B **51**, 279 (1983).
[19]E. Brezin, D. J. Gross, and C. Itzykson, Nucl. Phys. Ser. B **235**, 24 (1984).
[20]L. B. Ioffe and A. I. Larkin, Zh. Eksp. Teor. Fiz. **81**, 1048 (1981) [Sov. Phys. JETP **54**, 556 (1981)].
[21]I. Affleck, J. Phys. C **17**, 279 (1984).
[22]K. A. Benedict, Nucl. Phys. Ser. B **280**, 549 (1987).
[23]T. Ando and Y. Uemura, J. Phys. Soc. Japan **36**, 989 (1974); T. Ando, J. Phys. Soc. Jpn. **52**, 1740 (1983).
[24]J. Labbe, Phys. Rev. B **35**, 1373 (1987).
[25]A. H. McDonald, T. M. Rice, and W. F. Brinkman, Phys. Rev. B **28**, 3648 (1983).
[26]T. Ando, J. Phys. Soc. Japan **37**, 1616 (1974).
[27]T. Ando and Y. Murayama, J. Phys. Soc. Jpn. **54**, 1519 (1985).
[28]W. Cai and C. S. Ting, Phys. Rev. B **33**, 3967 (1986).
[29]T. Ando and Y. Uemura, J. Phys. Soc. Jpn. **37**, 1044 (1974).
[30]Y. Murayama and T. Ando, Phys. Rev. B **35**, 2252 (1987).
[31]R. R. Gerhardts and V. Gudmundsson, Phys. Rev. B **34**, 2999 (1986).
[32]B. I. Shklovskiĭ and A. L. Efros, *Electronic Properties of Doped Semiconductors*, Springer-Verlag (Springer Series in Solid-State Sciences, Vol. 45), New York, 1984 [Russ. original, Nauka, M., 1982].

[33]V. A. Gergel' and R. A. Suris, Zh. Eksp. Teor. Fiz. **84**, 719 (1983) [Sov. Phys. JETP **57**, 415 (1983)].
[34]S. Luryi, in: Proc. Intern. Conf. on Applied High Magnetic Fields in Semiconductor Physics, Wurzburg, ed. G. Landwehr, Sringer-Verlag (Springer Series in Solid-State Sciences, Vol. 71), New York, 1986, p. 24.
[35]B. I. Shklovskiĭ and A. L. Efros, Pis'ma Zh. Eksp. Teor. Fiz. **44**, 520 (1986) [JETP Lett. **44**, 669 (1986)].
[36]R. Peierls, Z. Phys. **81**, 186 (1933).
[37]V. M. Pudalov, S. G. Semenchinskiĭ, and V. S. Édel'man, Pis'ma Zh. Eksp. Teor. Fiz. **39**, 474 (1964) [JETP Lett. **39**, 576 (1984)].
[38]T. P. Smith, B. B. Goldberg, P. J. Stiles, and M. Heiblum, Phys. Rev. B **32**, 2696 (1988); Surf. Sci. **170**, 580 (1986).
[39]J. P. Eisenstein, H. L. Stormer, V. Narayanamurti, A. Y. Cho, and A. C. Gossard, Surf. Sci. **170**, 271 (1986); Superlatt. Microstruct. **11**, 1 (1985).
[40]J. P. Eisenstein, Appl. Phys. Lett. **46**, 695 (1985).
[41]V. M. Pudalov, S. G. Semenchinskiĭ, and V. S. Eidel'man, Zh. Eksp. Teor. Fiz. **89**, 1870 (1985) [Sov. Phys. JETP **62**, 1079 (1985)].
[42]V. M. Pudalov, S. G. Semechinskiĭ, and V. S. Edelman, Sol. State Commun. **51**, 713 (1984).
[43]V. M. Pudalov, S. G. Semenchinskiĭ, and V. S. Eidel'man, Pis'ma Zh. Eksp. Teor. Fiz. **41**, 265 (1985) [JETP Lett. **41**, 325 (1985)].
[44]I. M. Lifshitz and A. M. Kosevich, Zh. Eksp. Teor. Fiz. **29**, 730 (1988) [Sov. Phys. JETP **2**, 636 (1956)].
[45]M. I. Kaganov, I. M. Lifshitz, and K. D. Sinel'nikov, Zh. Eksp. Teor. Fiz. **32**, 605 (1957) [Sov. Phys. JETP **5**, 500 (1957)].
[46]N. E. Alekseevskiĭ and V. I. Nizhankovskiĭ, Zh. Eksp. Teor. Fiz. **83**, 1163 (1982) [Sov. Phys. JETP **56**, 661 (1982)].
[47]N. E. Alekseevskiĭ and V. I. Nizhankovskiĭ, Zh. Eksp. Teor. Fiz. **88**, 1771 (1985) [Sov. Phys. JETP **61**, 1051 (1985)].
[48]V. I. Nizhankovskiĭ, V. G. Mokerov, B. K. Medvedev, and Yu. V. Shaldin, Zh. Eksp. Teor. Fiz. **90**, 1326 (1986) [Sov. Phys. JETP **63**, 776 (1986)].
[49]R. T. Zeller, F. F. Fang, B. B. Goldberg, S. L. Wright, and F. J. Stiles, Phys. Rev. B **33**, 1529 (1986).
[50]D. Weiss, K. Klitzing, and V. Mossar, in: *Two-Dimensional Systems: Physics and New Devices*, ed. G. Baner, F. Kuchar, and H. Heinrich, Springer-Verlag (Springer Series in Solid State Sciences, Vol. 67), New York, 1986, p. 204.
[51]W. Zawadski and R. Lassnig, Surf. Sci. **142**, 225 (1984).
[52]R. Lassnig and E. Gornik, in: *Two-Dimensional Systems: Physics and New Devices*, ed. G. Baner, F. Kuchar, and H. Heinrich, Springer-Verlag (Springer Series in Solid State Sciences, Vol. 67), New York, 1986, p. 218.
[53]F. Stern, Phys. Rev. B **5**, 4891 (1972).
[54]V. Mosser, D. Weiss, K. Klitzing, K. Ploog, and G. Weimann, Solid State Commun. **58**, 5 (1986).
[55]D. C. Tsui, H. L. Störmer, and A. C. Gossard, Phys. Rev. B **25**, 1405 (1982).
[56]K. Klitzing, Festkörperprobleme **21**, 1 (1981).
[57]V. T. Dolgopolov and S. I. Dorozhkin, Poverkhnost' **4**, No. 2, 5 (1985) [Phys. Chem. Mech. Surf. **4**, 319 (1985)].
[58]M. G. Gavrilov and I. V. Kukushkin, Pis'ma Zh. Eksp. Teor. Fiz. **43**, 79 (1986) [JETP Lett. **43**, 103 (1986)].
[59]D. Weiss, E. Stahl, G. Weimann, K. Ploog, and K. Klitzing, Surf. Sci. **170**, 285 (1986).
[60]B. Tausenfreund and K. Klitzing, Surf. Sci. **142**, 220 (1984).
[61]A. A. Shashkin, V. T. Dolgopolov, and S. I. Dorozhkin, Zh. Eksp. Teor. Fiz. **92**, 1782 (1987) [Sov. Phys. JETP **65**, 999 (1987)].
[62]A. Hartstein and R. H. Koch, *Proc. of the 18th Intern. Conf. on the Physics of Semiconductors*, Stockholm, 1986, p. 481.
[63]W. Seidenbusch, R. Lassnig, E. Gornik, and G. Weimann, Proc. of the 18th Intern. Conf. on the Physics of Semiconductors, Stockholm, 1986, p. 593.
[64]Th. Englert, J. C. Maan, C. Vihlein, D. C. Tsui, and A. C. Gossard, Physica B **117/118**, 631 (1983).
[65] D. Heitmann, M. Ziesmann, and L. L. Chang, Phys. Rev. B **34**, 7463 (1986).
[66]I. V. Kukushkin and V. B. Timofeev, Pis'ma Zh. Eksp. Teor. Fiz. **40**, 413 (1984) [JETP Lett. **40**, 1231 (1984)].
[67]I. V. Kukushkin and V. B. Timofeev, Zh. Eksp. Teor. Fiz. **92**, 258 (1987) Sov. Phys. [JETP **65**, 146 (1987)].
[68]I. V. Kukushkin and V. B. Timofeev, Zh. Eksp. Teor. Fiz. **93**, 1088 (1987) Sov. Phys. [JETP **66**, 613 (1987)].
[69]A. B. Fowler, F. F. Fang, W. E. Howard, and P. J. Stiles, Phys. Rev. Lett. **16**, 901 (1966).
[70]R. Kummel, Zs. Phys. Kl. B **22**, 223 (1975).
[71]F. J. Ohkawa and Y. Uemura, J. Phys. Soc. Jpn. **43**, 907, 917 (1977).
[72]L. J. Sham and M. Nakayana, Phys. Rev. B **20**, 734 (1979); Surf. Sci. **73**, 272 (1973).
[73]F. J. Ohkawa and Y. Uemura, J. Phys. Soc. Jpn. **43**, 925 (1977).
[74]H. Ramh and R. Kummel, Surf. Sci. **98**, 370 (1980).
[75]I. V. Kukushkin, Pis'ma Zh. Eksp. Teor. Fiz. **45**, 222 (1987) [JETP Lett. **45**, 276 (1987)].
[76]G. A. Baraff and D. C. Tsui, Phys. Rev. B **24**, 2274 (1981).

Translated by A. Zaslavsky